FY2019 (2019.4-2020.3) NSEC
Annual Report

Nuclear Science and Engineering Center
Nuclear Science Research Institute, Sector of Nuclear Science Research
Japan Atomic Energy Agency

September 2020

Table of Contents

Preface

ENDO Akira

Director General, Nuclear Science and Engineering Center

The Nuclear Science and Engineering Center (NSEC) of the Japan Atomic Energy Agency (JAEA) aims to conduct research and development to advance the science and technology that supports the use of nuclear energy and radiation. This annual report provides research highlights and an overview of the research groups' activities in the NSEC for Fiscal Year 2019. We hope this annual report will increase your understanding of the NSEC.

The use of nuclear energy and radiation is supported by the underlying basic science and various technologies that link science and engineering. As such, we conduct fundamental research to elucidate various phenomena involving atomic nuclei, radiation, and radioactive materials using our innovative techniques for measurement and analysis. Based on modeling of the observed phenomena, we develop computer simulation codes and databases for predicting the behavior of energetic particles, heat and fluid in a reactor core, performance of nuclear fuel and reactor structural materials, properties and functions of radioactive materials related to their physical and chemical states, migration behavior of radionuclides in the environment, and the effects of radiation on the human body.

Through such knowledge and technologies, the NSEC contributes to solving various issues. Since the accident at the TEPCO Fukushima Daiichi Nuclear Power Plant, we have focused on research and development that contributes to (1) the accident response (promoting facility decommissioning and environmental restoration), (2) improvement of light water reactors' safety performance, and (3) steady implementation of the treatment and disposal of radioactive waste. Additionally, we disseminate our innovative technologies to resolve challenges in various fields, such as industry, environment and medicine.

In 2019, JAEA formulated a vision for the future, JAEA2050+, in order to identify our direction moving forward. To realize JAEA2050+, the NSEC will serve as a leading center for research collaboration and use our research and development capabilities to contribute to advances in science and technology. We seek your understanding, support, and encouragement in our research and development activities.

September 2020

FY2019 NSEC R&D Highlights

The following 6 highlights are selected among various outcomes of the R&D activities accomplished by the NSEC's 6 divisions in FY2019.

✓ **Nuclear Data and Reactor Engineering Division**:
 "Development of Photonuclear Data Library for International Contribution"

✓ **Fuels and Materials Engineering Division**:
 "Analysis for the Mechanism of Accelerated Corrosion on Low Alloy Steel in Air/solution Alternating Condition"

✓ **Nuclear Chemistry Division**:
 "External Exposure Dose Estimation by Electron Spin Resonance Technique for Wild Japanese Macaque Captured in Fukushima Prefecture"

✓ **Environment and Radiation Sciences Division**:
 "Warning System for Aviation Exposure to Solar Energetic Particles (WASAVIES)"

✓ **LWR Key Technology Development Division**:
 "Fission Product Chemistry Database ECUME for LWR Severe Accidents"

✓ **Partitioning and Transmutation Technology Division**:
 "New Experimental Data Obtained to Validate Nuclear Data for ADS"

Development of Photonuclear Data Library for International Contribution

IWAMOTO Nobuyuki

Nuclear Data Center

Photonuclear reaction is the phenomenon which happens when a nucleus is irradiated with high energy gamma-rays. Photonuclear data are basic ones not only for scientific researches but also for application fields. However, a large discrepancy is present between experimental data measured by the groups of the Lawrence Livermore National Laboratory in USA and the Saclay Nuclear Research Center in France, both of which led photonuclear researches in the 1960s to 80s. The discrepancy makes a big disadvantage on practical aspects such as the increase in the amount of radioactive waste due to a large uncertainty of inventory estimation. Therefore, the improvement of reliability of photonuclear data has been an overriding priority. The International Atomic Energy Agency (IAEA) started a coordinated research project (CRP) to develop a photonuclear data library in 2016, and the researchers of 15 countries participated. The present work was done within the framework of CRP.

From extensive application viewpoints, photonuclear data are required to cover wide gamma-ray energy and nuclide ranges. These requirements cannot be satisfied only by experiments. A nuclear reaction model is helpful for fixing the matter. We used up-to-date knowledge of theoretical reaction models and nuclear structure data. In the evaluation of photonuclear data, the key physical quantity is photon strength function, which represents the absorption and emission strengths of gamma-rays from nuclei. By analyzing experimental data in various gamma-ray energies and nuclides, we found out an optimum form of the photon strength function. This made photonuclear data calculated by the theoretical reaction models more reliable.

For the evaluation, we adopted the data measured by a research group of Romania, Norway, Russia and Japan in the CRP at the NewSUBARU facility in Japan, together with existing ones. The NewSUBARU experiments were devised to obtain accurate cross sections with a laser Compton scattering gamma-ray beam and a neutron detector with a flat detection efficiency. The use of these apparatuses gets rid of the primary factors of the discrepancy seen in the data of the above two groups.

Evaluations of 140 nuclides (e.g., structural and medium-heavy nuclides, and actinides) were performed in the gamma-ray energy range of 1 to 200 MeV. We obtained the photonuclear data which well reproduce the experimental data. In particular, the neutron emission cross sections were carefully improved in the giant dipole resonance region (10 to 20 MeV), where the cross sections are large. This improvement leads to the increase of practicality to many fields. The IAEA photonuclear data library 2019 includes the nuclear data of 219 nuclides from deuterium to Plutonium-241. Here, new 140 nuclides and existing 7 nuclides were provided from JAEA[1]. This library will be available from the website of IAEA Nuclear Data Services: https://www-nds.iaea.org/.

Figure 1 shows the comparisons of one- and two-neutron emission cross sections evaluated for Lanthanum-139 (^{139}La) with the data of NewSUBARU (circles), together with those of Saclay center (squares and triangles). The present results are in good agreement with the data of NewSUBARU. It is found that the data of Saclay center are lower than the present cross sections. It is inferred that the amount of undetected neutrons is large and the discrimination accuracy of neutron multiplicity is low. It is expected that the photonuclear data with an improved reliability largely contribute to the reduction in the amount of radioactive waste in electron accelerator facilities, and optimization of gamma-ray irradiation to human body on radiation therapy, in addition to contributing to the scientific researches.

Reference

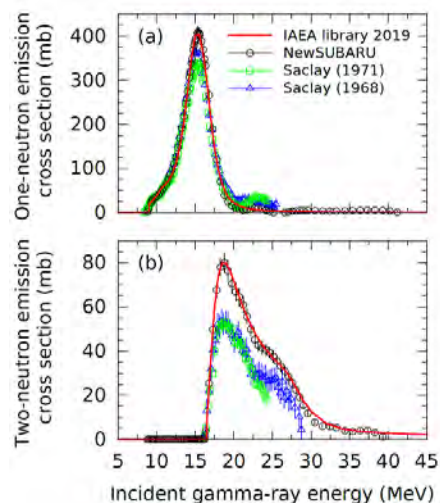1) T. Kawano et al., Nuclear Data Sheets, 163, 109-162 (2020).

Fig.1 Comparisons of (a) one-neutron and (b) two-neutron emission cross sections evaluated for ^{139}La with the data of NewSUBARU and Saclay center

Analysis for the Mechanism of Accelerated Corrosion on Low Alloy Steel in Air/solution Alternating Condition

OTANI Kyohei, TSUKADA Takashi, UENO Fumiyoshi and KATO Chiaki
Research Group for Corrosion Resistant Materials

In the TEPCO Fukushima Daiichi Nuclear Power Plant, it was observed that steel, the internal material of the reactor, was exposed to air/solution interface. It has been reported[1] that steel at the air/solution interface is exposed to a thin water film, and the corrosion rate is accelerated by the water film. In the present study, corrosion tests of carbon steel simulating the air/solution interface was carried out to clarify the mechanism of the accelerated corrosion[2].

For the corrosion tests simulating the air/solution interface, the carbon steel was rotated and exposed to air and solution alternately (interface condition) using a rotating corrosion test apparatus shown in Figure 1. The broken lines in Figure 1 mean the water level of the test solution. It was observed that a thin water film formed on the surface of the carbon steel during the test while it was exposed in the air. For comparison, corrosion tests were also carried out under the condition that the specimens were always immersed in the solution and rotated (immersion condition). 200 times diluted artificial seawater was used as the test solution. The cross-section of the rust layer and the mass change of the specimen were investigated after the tests.

The cross-sectional SEM images show that the rust layer formed on the steel after the tests in the interface condition was thicker than that of the immersion condition (Figure 2). The corrosion rate of carbon steel in the interface condition was more than three times larger than that of the immersion condition. It has been reported that the mass transfer of dissolved oxygen to the carbon steel surface is accelerated in case of the carbon steel covered by a thin water film and corrosion of carbon steel is accelerated by the acceleration of oxygen reduction reaction (cathodic reaction)[3]. This suggests that the accelerated corrosion of the steel in the interface condition would be caused by the thin water film on the steel during the tests.

The accelerated corrosion of carbon steel in the interface condition would be caused by the thin water film increasing mass transfer of dissolved oxygen to the carbon steel surface during the tests.

Reference

1) T. Nishimura et al., Tetsu-to-Hagane, **81**, 1079-1084, (1995). (in Japanese)
2) K. Otani et al., Zairyo-to-Kankyo, **68**, 205-211, (2019). (in Japanese)
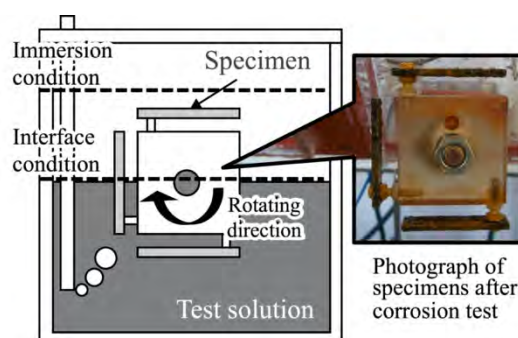3) A. Nishikata et al., J. Electrochem. Soc., **144**, 1244-1252, (1997).

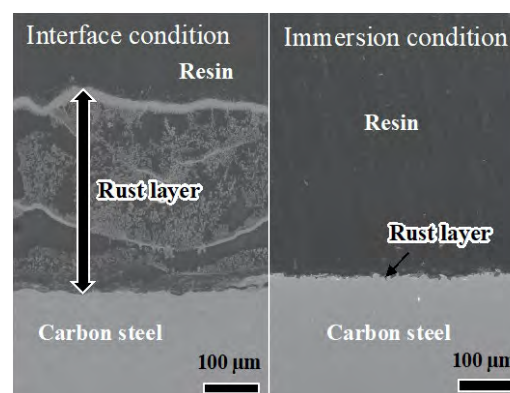**Fig.1 Schematic representation of the rotating corrosion test apparatus.**

Fig.2 Cross-sectional SEM images of the specimens tested in the interface condition and in the immersion condition.

External Exposure Dose Estimation by Electron Spin Resonance Technique for Wild Japanese Macaque Captured in Fukushima Prefecture

OKA Toshitaka

Research Group for Analytical Chemistry

The release of the radioactive materials from the TEPCO Fukushima Daiichi Nuclear Power Plant (1F) to the environment resulted in long-term low dose (below 100 mGy) exposure to humans/animals. From the viewpoint of biological effects and radiation safety for individuals, the precise exposure dose estimation is important.

Electron spin resonance (ESR) dosimetry is one of the powerful tools for exposure dose estimation. The principle of it is to measure the CO_2 radical, which was induced in tooth enamel by the radiation and retained with a lifetime more than 10^7 years (Figure 1). The relationship between exposure dose and CO_2 radical intensity, i.e., the dose response curve, enables us to estimate external exposure dose of the individuals. This technique was commonly applied for the high dose exposure estimation (from a few hundred mGy to a few Gy) for human, for example, exposure by atomic bomb, the nuclear plant accident in Chernobyl, the nuclear industry workers, and so on. The detection limit of the ESR dosimetry using human teeth was reported to be 100 mGy-200 mGy. To apply ESR dosimetry for the dose estimation due to 1F accident, improvement of the detection limit of ESR dosimetry is required. In the present study, we attempted to improve the detection limit using teeth of the Japanese macaque.

As reported in the previous study, organic materials in dentine will interfere with ESR measurement of CO_2 radical; it has been necessary to remove dentine and prepare dentine-free enamel samples[1]. However, because of the small size of macaque teeth, it is difficult to grind away with a dental bur. We attempted to remove dentine based on the difference in the density between enamel and dentine. Molar teeth of Japanese macaque were crushed into grains using a cryo-press, and enamel (density of 2.0-2.1 g/cm^3) was separated from dentine (density of 2.8 - 3.0 g/cm^3) by centrifugation.

To obtain the dose response curve, enamel samples were irradiated by ^{60}Co γ-ray up to 200 mGy (50, 100, 150, and 200 mGy) by cumulative irradiation. Before the first irradiation and after each irradiation, samples were measured by ESR to obtain a precise dose response curve (Figure 2). From this dose response curve, the detection limit is estimated to be less than 40 mGy.[1] Wild Japanese macaques captured at Namie town, Fukushima prefecture, about 15 km away from 1F were subjected to external dose estimation. We found out that some of them show the estimated

exposure dose below 100 mGy.

The improved detection limit will enable us to examine the relationship between external radiation doses (at least 40 mGy) and their biological effects not only on wild Japanese macaques but also on Japanese field mice and raccoons in Fukushima prefecture. One of our goals is to assess the exposure radiation dose for children in Fukushima prefecture.

Reference

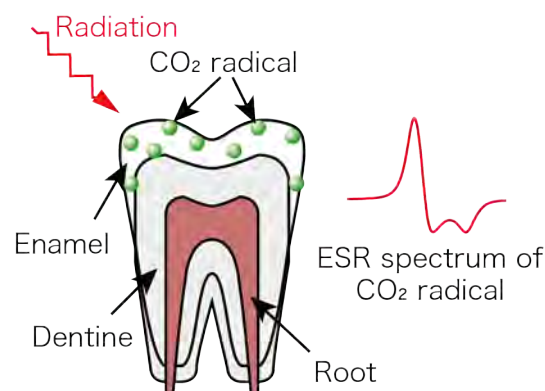1) T. Oka et al., Radiation Measurements, 134, 106315-1--4 (2020).

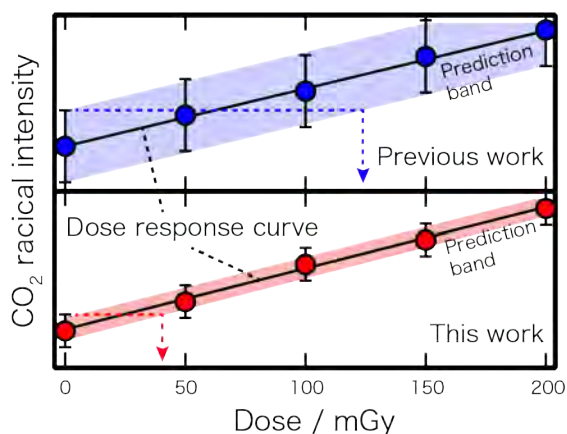**Fig.1 CO$_2$ radicals induced by radiation. Measure the CO$_2$ radical intensity by ESR spectrometer.**

Fig.2 Dose response curve for tooth enamel. Purple and red bands represent the 90 % prediction bands of each curve. This work can estimate the lower exposure dose than the previous work.

Warning System for Aviation Exposure to Solar Energetic Particles (WASAVIES)

SATO Tatsuhiko[1], KATAOKA Ryuho[2], SHIOTA Daiko[3], KUBO Yuki[3], ISHII Mamoru[3], YASUDA Hiroshi[4], MIYAKE Shoko[5], PARK Inchun[6], MIYOSHI Yoshizumi[6]

1 Research Group for Radiation Transport Analysis, 2 National Institute of Polar Research, 3 National Institute of Information and Communications Technology, 4 Hiroshima University, 5 National Institute of Technology, Ibaraki College, 6 Nagoya University

When a large solar flare occurs, the radiation doses due to solar energetic particles (SEP) are occasionally increased especially at flight altitudes, and they can be a potential hazard to aircrews and passengers. Thus, development of a system for nowcasting and/or forecasting radiation doses due to SEP exposure is one of the most important challenges in space weather research. Collaboration with other research fields such as nuclear physics and radiological protection is the key issue in such development.

We therefore developed a physics-based model for SEP dose estimation anywhere in the atmosphere and designated it WASAVIES: WArning System for AVIation Exposure to Solar energetic particles[1], under the collaboration between several institutes in Japan. This system is based on the combination of SEP transport simulation models from the Sun to the ground level of the Earth. JAEA was responsible for developing the SEP transport simulation model in the atmosphere based on PHITS and the automatic analysis program by integrating all of the models.

The performance of WASAVIES is examined by analyzing the four major solar particle events of the 21st century. The accuracy of the nowcast data obtained by the model is well validated by the reproducibility of the ground and satellite observations. Figures 1 and 2 show the worldwide dose rate map at 12 km and route-dose rate map between Tokyo and New York, respectively, during the peak of the solar particle event occurred on Jan. 20, 2005 drawn using WASAVIES. The complicated latitude, longitude, and altitude dependences of the dose rates such as the southern asymmetry can be seen in these figures, owing to the sophisticated physics models implemented in WASAVIES.

A web-interface of WASAVIES was also developed and opened via public server of National Institute of Information and Communications Technology (NICT) (https://wasavies.nict.go.jp/) since Nov. 7th, 2019. The radiation dose during a large solar flare calculated by WASAVIES will be used as mandatory information for aviation operation management by International Civil Aviation Organization (ICAO). This study is a successful example of interdisciplinary research that has been achieved through collaboration among researchers in various fields such as space weather, solar physics, upper atmosphere physics, nuclear physics, and radiation protection. This work was partially supported by JSPS grant KAKENHI 15H05813.
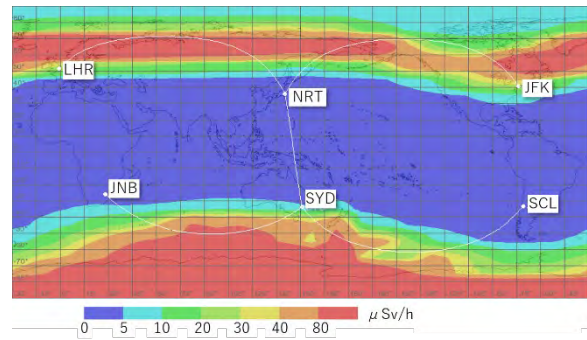
Fig.1 Worldwide dose rate map at 12 km at the peak of the largest solar particle event occurred on Jan 20, 2005 drawn using WASAVIES

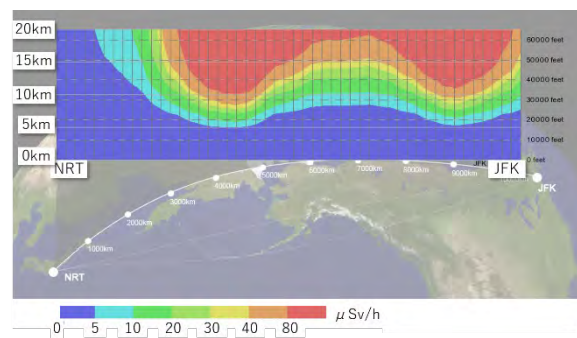**Fig.2 Route-dose rate map between Tokyo (NRT) and New York (JFK) at the peak of the largest solar particle event occurred on Jan 20, 2005 drawn using WASAVIES**

Reference

1) T. Sato et al., Real-Time and Automatic Analysis Program for WASAVIES: Warning System for Aviation Exposure to Solar Energetic Particles, Space Weather, 16, 924-936 (2018).

Fission Product Chemistry Database ECUME for LWR Severe Accidents

MIWA Shuhei, NAKAJIMA Kunihisa, SUZUKI Chikashi, SUZUKI Eriko, LIU Jiazhan, Imoto Junpei, KARASAWA Hidetoshi and OSAKA Masahiko

Development Group for LWR Advanced technology

Improvement of source term under LWR severe accidents (SAs) is of crucial importance both for the enhancement of LWR safety and the decommissioning and dismantling of the TEPCO Fukushima Daiichi Nuclear Power Plant (1F). One of the main tools for the evaluation of source term is an SA analysis code. Implementation of fission product (FP) chemistry treatment to the SA analysis code has been the effective and promising way for the improvement of source term. This is because the FP chemistry significantly influences all the FP behaviors.

Thus, we have been conducting a fundamental study for constructing the FP chemistry database named "ECUME" (Effective Chemistry database of fission products Under Multiphase rEaction)[1]. ECUME consists of three kinds of datasets: CRK (dataset for Chemical Reaction Kinetics), EM (Elemental Model set) and TD (ThermoDynamic dataset). ECUME version 1.1 has been developed in order to contribute mainly to the evaluation of Cs distribution in 1F. Namely, the following datasets were developed for evaluation of the effects of boron (BWR control material) on Cs chemistry and Cs chemisorption onto stainless steel (SS) at upper part of the reactor pressure vessel: CRK for the reaction of Cs-I-B-Mo-O-H system in gas phase, EM for Cs chemisorption onto SS caused by the high temperature reaction between Cs and Fe, Si, and TD for $CsBO_2$ vapor and solid $Cs_2Si_4O_9$ and $CsFeSiO_4$. ECUME is the first database for Cs-I-B-Mo-Fe-Si-O-H system in the world applicable to the evaluation of FP chemical reaction kinetics.

The constants in CRK have been prepared by a combination of an ab-initio calculation and literature review. A simulation calculation of Cs-I-B-Mo-O-H system with the presently prepared CRK in a simple thermal-hydraulic condition has revealed the necessity of application of chemical reaction kinetics instead of the chemical equilibria that has been used so far (Figure 1)[2].

The improved model for Cs chemisorption onto SS in EM has successfully reproduced the effects of various chemical conditions such as CsOH vapor concentration in gas phase and Si content in SS, which were not able to be evaluated by the existing model. The improved model shows that the existing model may significantly over/under-estimate Cs chemisorption rate according to various chemical conditions that should have appeared reactors in Unit 1-3 at 1F[2].

Thermodynamic data for $CsBO_2$ vapor with high accuracy were derived from the experiments, which were also conducted by ourselves. Thermodynamic data for solid $Cs_2Si_4O_9$ and $CsFeSiO_4$ were prepared for the first time in the world by the experiment and the DFT based calculation, respectively.

ECUME version 1.1 was successfully constructed for the evaluation of Cs distribution in 1F. In addition, ECUME version 1.1 includes the datasets for the evaluation of source term in PWR SA such as CRK for the reaction of Ru-N-O-H system in gas phase. In the future, ECUME will be expanded for more accurate evaluation of FP behaviors under the LWR SA. Thus, it can be expected to provide the fundamental solution for the issues towards the enhancement of LWR safety and the 1F decommissioning and dismantling work.

Reference

1) Development Group for LWR Advanced technology, JAEA-Data/code 2019-017 (2020).
2) S. Miwa et al., Mech. Eng. J., 7(3), 19-00537, (2020).
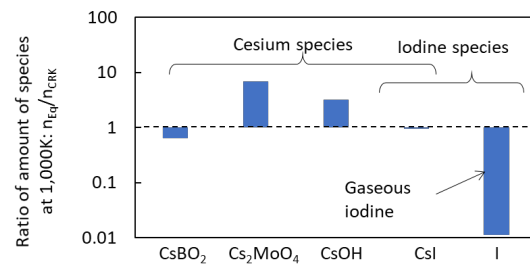
n_{Eq}: amount of species analyzed by chemical equilibrium calculation
n_{CRK}: amount of species analyzed by reaction calculation with CRK

Fig.1 Effect of application of chemical reaction kinetics on amount of Cs and I species (n_{Eq}/n_{CRK}).

New Experimental Data Obtained to Validate Nuclear Data for ADS

OIZUMI Akito, FUKUSHIMA Masahiro and NISHIHARA Kenji

Research Group for Nuclear Transmutation System

A fast neutron system dedicated to transmutation (accelerator-driven system: ADS) has been investigated to reduce the environmental burden of high-level radioactive waste (HLW). ADS is capable of converting partitioned long-lived nuclides with strong radiotoxicity into stable or short-lived nuclides by fission reaction with neutrons. The top candidate for ADS coolant is lead bismuth, which is chemically stable and highly safe. However, Japan has no experience with the use of lead bismuth as a nuclear reactor coolant, and the characteristics of the nuclear reaction (nuclear-reaction cross section) of lead have not been sufficiently verified. Hence, in this study, the new experimental data were obtained to validate the nuclear-reaction cross section of lead in fast neutron cores using a critical assembly in the United States.

In ADS, fast neutrons generated by the spallation reaction of lead-bismuth target are gradually moderated by nuclear reaction with lead-bismuth coolant, leading to fission after being absorbed to long-lived nuclides. Fast neutrons generated by the fission are also used for the next fission reaction through a similar moderation process (fission chain reaction). Thus, to correctly predict the neutron-mediated fission chain reaction in ADS, it is important to accurately evaluate the nuclear-reaction cross section of lead that affects neutron moderation in the coolant. Because moderation of fast neutrons exhibits different tendencies for different types of fuel, verification in several kinds of fuel is effective and reliable.

To verify the cross section of lead, influence of removing (voiding) the lead from an experimental core on fission chain reaction is measured. The influence is called "lead-void-reactivity worth". By voiding lead, neutrons are less moderated and keep at high speeds. Such neutrons tend to cause more fission in a core with particular fuel, or to escape from one core into another one. This different tendency among the fuel characteristics results in accurately measurable value, i.e., criticality (reactivity) of the core and is worth to verify the cross section of lead. The two experimental cores with different uranium (U) isotope ratios, a highly-enriched uranium (HEU)/lead-experimental core rich in ^{235}U and a low-enriched uranium (LEU)/lead-experimental core rich in ^{238}U, had been constructed in this experimental series so far. Recently, a new measurement was conducted by using a plutonium (Pu) /lead-experimental core in the same way as the experiments using U[1].

In the Pu fuel, neutrons moderated by lead generally have a higher probability of fission than unmoderated fast neutrons. Therefore, the removing lead from the Pu/lead experimental core decreases the amounts of moderated neutrons by escaping from the core and then the fission chain reaction becomes less likely to occur. This resulted in a negative lead-void-reactivity worth (Figure 1). These measurements were compared with the calculation values using nuclear-reaction cross section data (nuclear data) developed in Japan (JENDL-4.0) and the United States (ENDF/B-VIII.0). As a result, the calculation results using ENDF/B-VIII.0 well reproduced the experimental ones, whereas that using JENDL-4.0 overestimated them by almost 6 cents in absolute value. Further analysis of the gap between both calculations using JENDL-4.0 and ENDF/B-VIII.0 indicated that the fundamental cause was due to the difference in the nuclear data of one of Pu isotope, ^{239}Pu, and not that of lead.

By this study, the experimental data using Pu were added to a series of experiments for reliable validation of the nuclear-reaction cross sections of lead. The research group of Japan and the United States will continue the cooperation to advance the research and development on transmutation technology by expanding experimental data for validating the nuclear-reaction cross section.

This research was conducted as part of a collaboration with the Los Alamos National Laboratory in the United States.

Reference

1) M. Fukushima, J. Goda, A. Oizumi et al., Nuclear Science and Engineering, 194(2), pp.138-153 (2020).
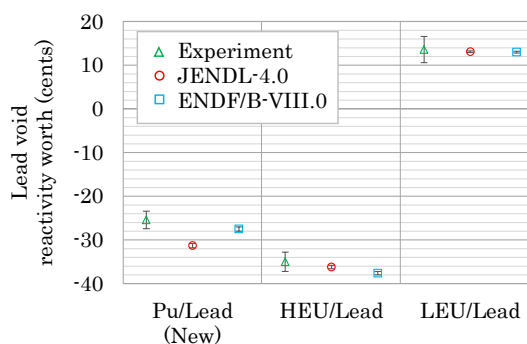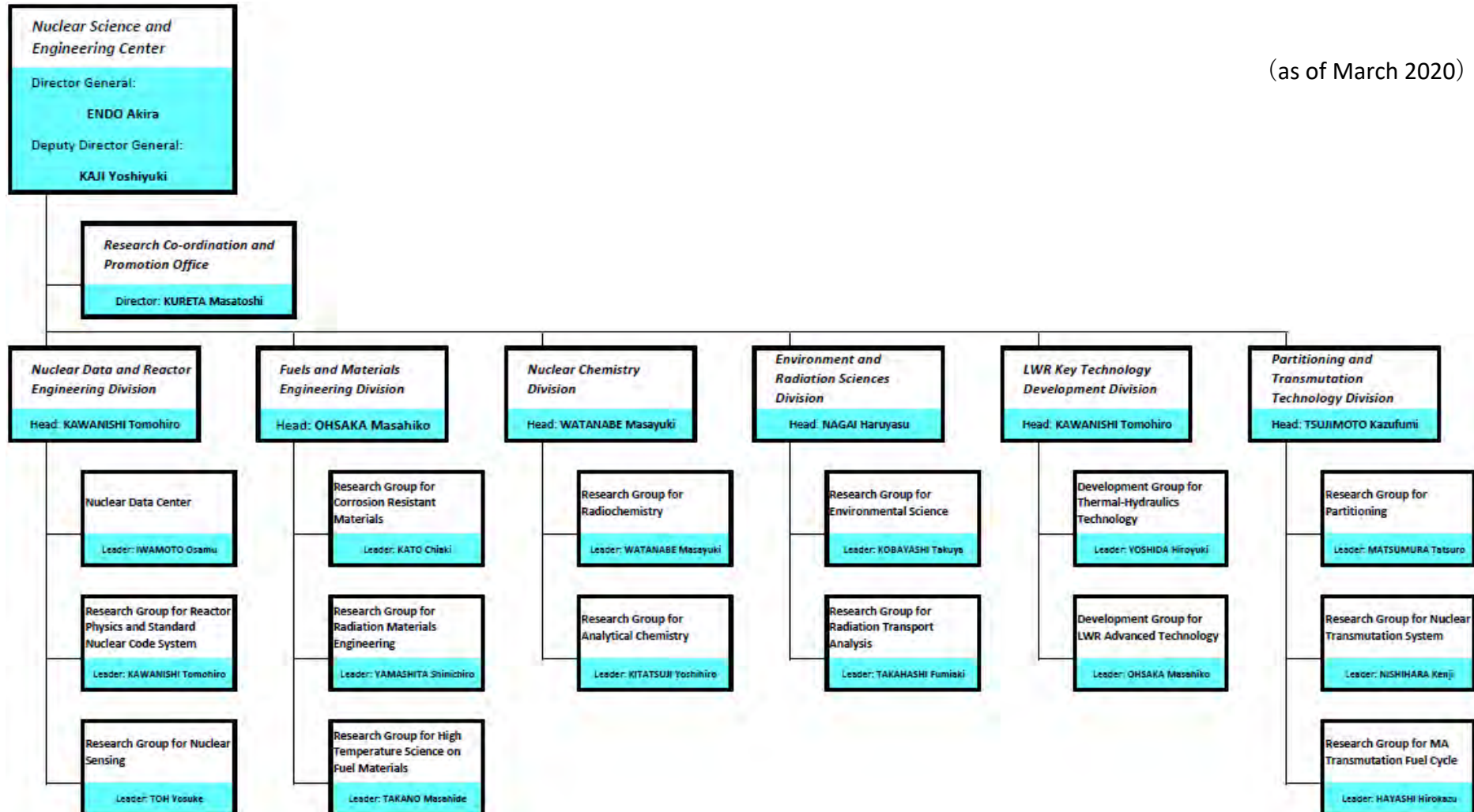
Fig.1 Comparison of experimental and calculated lead-void-reactivity worth

FY2019 NSEC Group Activities

The NSEC of JAEA consists of 15 Groups.

Organization of NSEC in FY 2019

（as of March 2020）

Nuclear Science and Engineering Center
Director General:
ENDO Akira
Deputy Director General:
KAJI Yoshiyuki

Research Co-ordination and Promotion Office
Director: KURETA Masatoshi

Nuclear Data and Reactor Engineering Division
Head: KAWANISHI Tomohiro

- Nuclear Data Center
  Leader: IWAMOTO Osamu
- Research Group for Reactor Physics and Standard Nuclear Code System
  Leader: KAWANISHI Tomohiro
- Research Group for Nuclear Sensing
  Leader: TOH Yosuke

Fuels and Materials Engineering Division
Head: OHSAKA Masahiko

- Research Group for Corrosion Resistant Materials
  Leader: KATO Chiaki
- Research Group for Radiation Materials Engineering
  Leader: YAMASHITA Shinichiro
- Research Group for High Temperature Science on Fuel Materials
  Leader: TAKANO Masahide

Nuclear Chemistry Division
Head: WATANABE Masayuki

- Research Group for Radiochemistry
  Leader: WATANABE Masayuki
- Research Group for Analytical Chemistry
  Leader: KITATSUJI Yoshihiro

Environment and Radiation Sciences Division
Head: NAGAI Haruyasu

- Research Group for Environmental Science
  Leader: KOBAYASHI Takuya
- Research Group for Radiation Transport Analysis
  Leader: TAKAHASHI Fumiaki

LWR Key Technology Development Division
Head: KAWANISHI Tomohiro

- Development Group for Thermal-Hydraulics Technology
  Leader: YOSHIDA Hiroyuki
- Development Group for LWR Advanced Technology
  Leader: OHSAKA Masahiko

Partitioning and Transmutation Technology Division
Head: TSUJIMOTO Kazufumi

- Research Group for Partitioning
  Leader: MATSUMURA Tatsuro
- Research Group for Nuclear Transmutation System
  Leader: NISHIHARA Kenji
- Research Group for MA Transmutation Fuel Cycle
  Leader: HAYASHI Hirokazu

URL of Organization of NSEC from April, 2020 (FY2020) : https://nsec.jaea.go.jp/organization/en_index.html

Nuclear Data Center

The mission of Nuclear Data Center is to provide reliable nuclear data which are required in various applications such as nuclear reactors, accelerators, medical use of radiations, and so on. To achieve that, we engage in research works on nuclear data measurement, nuclear theories, and nuclear data evaluation related to nuclear reaction and structure, collaborating with nuclear data researchers and organizations in Japan as well as in the world. The evaluated nuclear data have been compiled into databases called JENDL and are available from our website http://wwwndc.jaea.go.jp.

JENDL/ImPACT-2018*

To provide reliable data for the conceptual design of transmutation system of long-lived fission products (LLFPs) using accelerators that was carried out under a project of the ImPACT Program in Japan, a JENDL special purpose file JENDL/ImPACT-2018[1] was developed and released in August of 2019. With refining the theoretical models based on the newly obtained experimental data in the project, the nuclear data evaluations for JENDL/ImPACT-2018 were performed by applying the state-of-the-art theoretical model codes taking account of the currently available experimental data. The file contains cross sections of neutron and proton induced reactions up to 200 MeV on 163 nuclides: LLFPs and their surrounding nuclei which are expected to be produced during transmutations. These data were contributed to the reliable estimation of amount of various reaction products as well as neutron and proton transportation in the transmutation systems.

Hybrid Level Density Model*

Level density represents the average number of levels of nuclei at certain excitation energies, which play a crucial role on theoretical estimation of nuclear reaction cross sections. A new phenomenological model, which shows good agreements with experimental data for various type of nuclei having from spherical shapes to deformed ones, has been proposed[2]. The model consists of hybrid parametrizations of spherical and deformed formulations and they are optimized with existing experimental information on the spherical and deformed nuclei in cooperation with microscopic theoretical predictions of nuclear deformation depending on excitation energies. This model was applied to the evaluations for JENDL/ImPACT-2018.

Measurements of ^{237}Np and ^{243}Am Cross Sections**

Neutron cross sections of ^{237}Np and ^{243}Am have been measured by activation and time of flight (TOF) methods, respectively. These nuclides are some of the main components of nuclear wastes in spent fuels and accurate nuclear data have been required.

Regarding ^{237}Np, the thermal capture cross section and the resonance integral have been obtained from the irradiated samples using Gd filers instead of usual Cd ones, which enable us to remove effects of low-energy resonance existed in ^{237}Np leading to reliable estimation[3].

The capture and total cross sections of ^{243}Am have been measured using ANNRI facility at J-PARC[4]. The intensive pulsed neutron source of MLF of J-PARC enables measurement of cross sections with small amounts of samples which is crucial in use of minor actinide targets such as Np and Am. The final results were obtained for neutron energies from 10 meV to 100 eV and from 4 meV to 100 eV for capture and total cross sections, respectively.

Reference

1) S. Kunieda et al., J. Nucl. Sci. Technol, 56, 1073-1091 (2019).
2) N. Furutachi et al., J. Nucl. Sci. Technol, 56, 412-424 (2019).
3) S. Nakamura et al., J. Nucl. Sci. Technol, 56, 493-502 (2019).
4) A. Kimura et al., J. Nucl. Sci. Technol, 56, 479-492 (2019).

Contact (Group Leader):
IWAMOTO Osamu
iwamoto.osamu@jaea.go.jp

Research Group for Reactor Physics and Standard Nuclear Code System

The role of nuclear codes is increasing because of rapid advancement of computer technology. It enables to evaluate in detail the energy and spatial distribution of neutrons and photons emitted after fission reactions in a nuclear reactor. Important key properties such as criticality and radioisotope production rate etc. can be deduced from these neutronics calculations by these nuclear codes.

We are developing standard nuclear codes to support and advance nuclear energy and technology. The main codes are MVP and FRENDY. We are also collaborating tightly with the JENDL project and preparing many cross section libraries. We prepared a multi-group neutron activation cross-section library (MAXS/AD-2017) and developed inventory calculation modules for decommissioning of nuclear power plants in 2019 JFY.

MVP

MVP realizes fast and accurate Monte Carlo simulation of neutron and photon transport processes. The version 3 of MVP[1] was released in August 2018 and available from RIST in Japan and OECD/NEA data bank as NEA-1673 MVP/GMVP V.3. The cross section libraries for MVP3 can be downloaded from our group's home page.[2]

FRENDY

FRENDY is a nuclear data processing code[3]. It enables processing of nuclear data such as JENDL. The first version of FRENDY treats the ENDF-6 format and generates the ACE files which are used for Monte Carlo codes such as PHITS and MCNP. FRENDY-1 was released in March 2019 as an open source code from our group's home page[2].

MAXS/AD-2017

JENDL Activation Cross Section File for Nuclear Decommissioning 2017 (JENDL/AD-2017)[4] was released in 2018. MAXS/AD-2017 with the same format as MAXS-2015[5], which was produced based on the nuclear data libraries JENDL-4.0 and JEFF-3.0/A, was developed from JENDL/AD-2017 for activation calculations in nuclear facility decommissioning. A simple code to generate an ORIGEN-S library from MAXS/AD-2017 was also produced. JPDR activation analyses with ORIGEN-S[6] and a library generated from MAXS/AD-2017 demonstrated that MAXS/AD-2017 has a performance equivalent to the ORIGEN-S library in SCALE6.0.

Development of Inventory Calculation Modules

Radiological characterization is required as one of the preparatory tasks for decommissioning of nuclear power plants. We developed inventory calculation modules[7] using ORIGEN-S for reliable evaluations of radioactivity inventory collaborated with the Japan Atomic Power Company and the Institute of Applied Energy. As shown in Figure 1, an activation cross-section data library for ORIGEN-S is updated easily and effectively based on a facility-specific neutron spectrum and MAXS files by using these modules. We can mitigate mistakes in data handling around ORIGEN-S calculations.

Reference
1) Y. Nagaya et.al., JAEA-Data/Code, 2016-018 (2017).
2) https://rpg.jaea.go.jp/main/en/program/ (accessed 2020-05-22).
3) K. Tada et al., JAEA-Data/Code, 2018-014 (2019).
4) https://wwwndc.jaea.go.jp/ftpnd/jendl/jendl-ad-2017. html (accessed 2020-05-22).
5) K. Okumura et al., JAEA-Conf 2015-003, p. 43 (2016).
6) I.C. Gauld et al., ORNL/TM-2005/39 (2006).
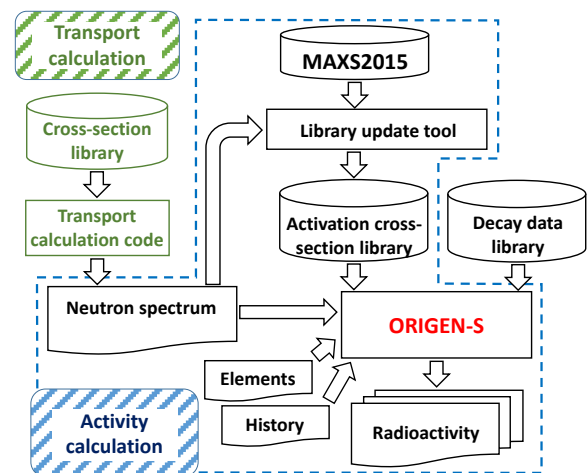7) N. Matsuda et al., JAEA-Data/Code 2020-003 (2020).

Fig. 1 Example of inventory calculation modules

Contact (Group Leader):
KAWANISHI Tomohiro
kawanishi.tomohiro@jaea.go.jp

Research Group for Nuclear Sensing

We are dedicated to the research and development of radiation measurement techniques and systems and those applications. In particular, non-destructive analysis (NDA) that requires advanced neutron measurement techniques has been developed and could be an indispensable tool for nuclear safeguards, nuclear security, nuclear waste management and decommissioning. Developments of low-cost, accurate and practical NDA systems are also needed for effective implementation. The following are a part of our group activities in 2019.

Fast Neutron Direct Interrogation

We have developed the Fast Neutron Direct Interrogation (FNDI) that is an NDA technique for nuclear materials. FNDI is a kind of Differential Die-Away Analysis (DDA). The conventional DDA uses thermal neutrons for sample interrogation. By contrast, FNDI utilizes fast neutrons for interrogation to reduce the influence of sample matrices. As a result, FNDI can measure a variety of nuclear materials nondestructively and enable us to rapidly and accurately measure a small amount of fissile materials in a nuclear waste drum. We applied it in the accountancy of 1802 actual waste drums generated in decommissioning of a nuclear facility. A low-cost and transportable neutron source has also been developed to improve the capability of an NDA system[1] (Figure 1). M. Kureta, A. Ohzu and M. Komeda were awarded the MEXT Minister Prizes for Science and Technology for their work on the implementation of the novel NDA system by using the FNDI[2].
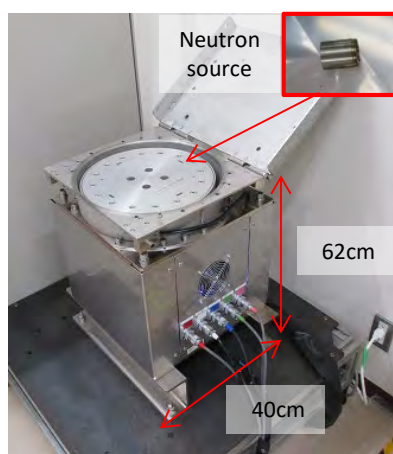

Fig. 1 Low-cost neutron apparatus. We have successfully demonstrated the detection of nuclear materials with the low-cost neutron apparatus.

Neutron Resonance Transmission Analysis

Neutron cross sections show resonance structures that can be used in the identification and quantification of nuclides. Neutron Resonance Transmission Analysis (NRTA) is based on the analysis of the resonance structures and is one of the most promising NDA techniques. In particular, NRTA can be applied for highly radioactive materials because the detector of NRTA is located far away from the radioactive materials.

The specially designed large-volume $LaBr_3$ detector system for NRTA was developed and evaluated[3]. The neutron energy spectra obtained by the $LaBr_3$ detector system showed that prompt γ ray peaks emitted from standard samples can be used to accurately identify the nuclei. Moreover, the signal-to-noise ratios of resonance peaks in the spectrum were enhanced 1.5–2.5 times by using the $LaBr_3$ detector system.

We also established the analytical techniques for NRTA to handle complex nuclear material samples such as spent nuclear fuel pellets[4]. It was implemented in the resonance shape analysis code and was validated by experiments at the time-of-flight facility GELINA using a set of metallic natural copper samples and pellets made of silver mixed with uranium-oxide powder. The results of the experiments reveal that sample properties can be derived even when ideal geometry conditions are not fulfilled. The analytical techniques open perspectives to apply NRTA as an absolute analytical NDA technique to determine the elemental and isotopic compositions of complex nuclear materials.

This research was implemented under the subsidy for nuclear security promotion of MEXT.

Reference

1) M. Komeda and Y. Toh, J. Nucl. Sci. Technol., 56, 617-628 (2019).

2) M. Kureta, A. Ohzu and M. Komeda, The Commendation for Science and Technology by MEXT, April 9 (2019).

3) H. Tsuchiya et al., Nucl. Instr. Meth. A 932, 16-26 (2019).

4) F. Ma et al., J. Anal. At. Spectrom., 35, 478-488 (2020).

Contact (Group Leader):

TOH Yosuke

toh.yosuke@jaea.go.jp

Research Group for Corrosion Resistant Materials

Our group studies the corrosion of materials used in light water reactors, spent fuel reprocessing plants, ADS (Accelerator Driven System). We mainly conduct corrosion tests in non-radioactive environments and in radioactive environments to elucidate the mechanisms of corrosion phenomena and prediction models for corrosion. We also use computer science to understand and predict corrosion mechanisms in areas that are difficult to see due to the experimental limitations.

Hydrogen Permeation Mechanism into Iron simulated by First-principles Calculation Analyses[1]

Hydrogen embrittlement is a phenomenon in which the strength of steel is reduced by the hydrogen absorbed in the steel. There are microscopic defects in structural materials in nuclear reactors due to irradiation. These defects have a possibility of capturing hydrogen and then cause hydrogen embrittlement. In order to obtain the basic mechanism of hydrogen permeation into metal, first-principles calculations were conducted to acquire the adsorption potential of the metal cations (Na^+, Mg^{2+}, and Zn^{2+}) in solution, E_{ad}, and the electron density difference between before and after metal cation adsorption at the point of zero-charge, $\Delta\rho$, which were derived from the electronic state around the iron surface. E_{ad} was derived using follow equation,

$$E_{ad} = -\Delta G/nF$$

where G, n and F represent Gibbs free energy, the number of reacted electrons, and Faraday constant, respectively. ΔG represents the difference in free energy before and after the reaction,

$$\Delta G = G(\text{Fe}_{slab} + \text{M}_{ad})$$
$$-\{G(\text{Fe}_{slab}) + G(\text{M}^{n+})\}$$

where M represents the investigated metal species (= Na, Mg, Zn). $\Delta\rho$ was derived using follow equation,

$$\Delta\rho = \rho_{\text{FeSlab}+M} - (\rho_{\text{FeSlab}} + \rho_M)$$

where $\rho_{\text{FeSlab}+M}$, ρ_{FeSlab}, and ρ_M represent electron density of the iron slab with metal cation adsorption, that of the iron slab, and that of the metal cation, respectively. Fig. 1 shows a contour plot of electron density difference around adsorbed atom at point of zero charge. Fig. 2 shows the electron density difference of each cation as a function of relative position between nearest Fe atom and cation; $r_{\text{Fe-M}}$ / $L_{\text{Fe-M}}$, where $r_{\text{Fe-M}}$ and $L_{\text{Fe-M}}$ represent position from Fe atom

and distance between Fe and cation, respectively. As shown in these figures, for Zn, which had a large adsorption potential, obvious increase in electron density between adsorbed atom and Fe at surface were observed. On the other hand, no significant increase in electron density was observed for Na. For Mg, increase in the electron density was shown in Figure 1, but there was large negative electron density difference near Mg atom, that is, weak binding force. That was obviously different from Zn, and seems to be anti-chemical bonding. It was suggested that the dissolution reaction of iron was suppressed by the formation of the Zn layer, and that lead suppression of hydrogen permeation into iron. These results were in good agreement with experimental data. This study is expected to contribute to clarifying the hydrogen embrittlement mechanism of structural materials of nuclear facilities.
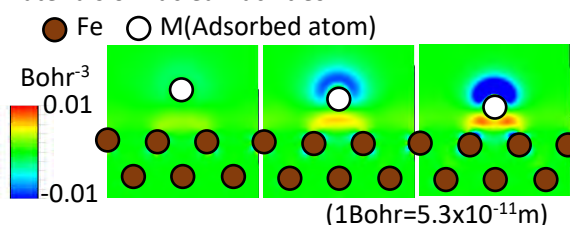

(1Bohr=5.3×10^{-11}m)

Fig.1 Contour maps of electron density difference around each adsorbed atom of (a) Na, (b) Mg and (c) Zn.
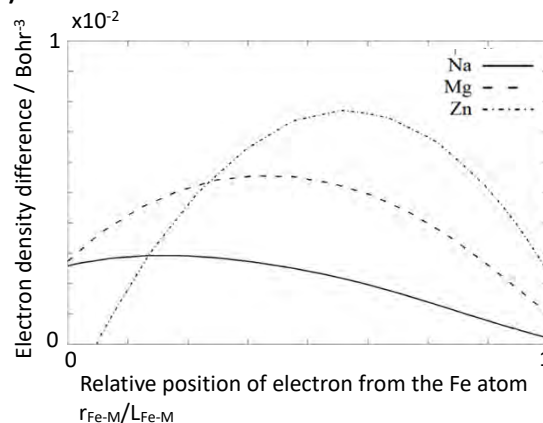

Fig.2 Distribution of electron density difference between the adsorbed atom and the nearest Fe atom.

Reference
1) T. Igarashi et.al., ISIJ International, accepted.

Contact (Group Leader):
KATO Chiaki
Kato.chiaki16@jaea.go.jp

Research Group for Radiation Materials Engineering

We are conducting several researches related to not only the material degradation mechanism under radiation environment but also the development of novel analytical methods expected to be applied to nuclear materials. As one of the studies developing the novel analytical methods, we just started to apply Positron Annihilation Spectroscopy (PAS) for the study of Room Temperature Ionic Liquids (RTILs), which are expected to be applied for the reprocessing of spent nuclear fuel. In addition, we are also investigating the effects of the irradiation- defect motion on the microstructural evolution by combining the experimental and modeling techniques to improve the prediction accuracy of the property changes in irradiated materials for ensuring the integrity of nuclear reactors.

Application of the PAS for the Study of RTILs.

Although RTILs are widely used, indirect methods are often used for physical property evaluation in the nano or sub-nano scale. Positronium (Ps), which is a combination of positron and electron, can be a nano or sub-nano probe. Ps can form a sub-nano bubble and localize there because of its negative work function and the triplet Ps (ortho-Ps) lives longer in a larger Ps bubble. In the usual molecular liquids, the expansion of Ps bubbles at higher temperatures were observed because of the smaller surface tension. In the previous studies, the Ps bubble in RTIL's showed some new phenomena like GHz oscillation that was not observed in the usual molecular liquids and it was suggested that the Ps bubble size can show the size of the nano or sub-nano structure composed of the Coulomb force in RTIL's. Hence, no increase of ortho-Ps lifetime at higher temperatures was predicted. The temperature dependence of the positron lifetime at the near-surface and in the bulk of the RTIL was measured by the beam that can inject positrons from above the liquid surface at AIST[*] and the prediction was confirmed (Figure 1). It was also found that the structure due to the Coulomb force existing at the near-surface can remain even at high temperatures [1].

[*] AIST: National Institute of Advanced Industrial Science and Technology

In situ Observation of Irradiation-Defect Motion and its Modeling

Motion behavior of irradiation defects is known to affect the radiation-induced microstructural evolution and the degradation of material properties in crystalline materials. By in situ observation using electron microscopy, we revealed a fundamental defect-motion mechanism, i.e. trapping/detrapping by impurity atoms, in pure iron. Based on the revealed mechanism, we derived the analytical model using a random walk theory, and incorporated it into a reaction rate theory. Figure 2 shows how the evolution behavior of the irradiation-defect density depends on the impurity concentration in pure iron. The decreasing behavior was in a closer accordance with the experimental data with the impurity concentration $C_M = 10^{-5}$-10^{-4}, as experimentally deduced. This result suggests that the revealed motion mechanism is a fundamental physical process under irradiation[2].

Reference
1) T. Hirade, et al., ACTA PHYSICA POLONICA A, 137 109-112 (2020).
2) Y. Abe, et al., Philosophical Magazine, Vol. 100, pp. 110-125 (2020).

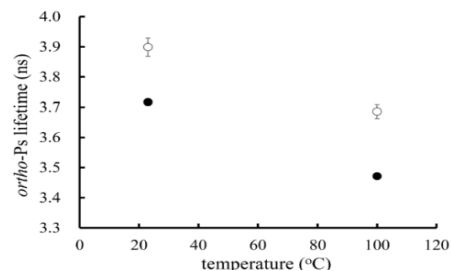**Fig.1 Temperature dependence of *ortho*-Ps lifetimes measured with positron energies of 2 keV (filled circles) and 12 keV (open circles).**
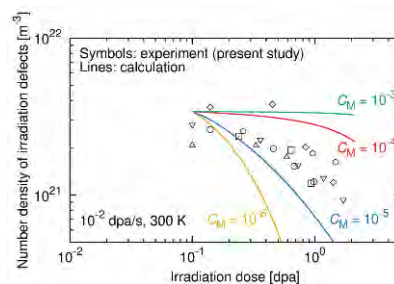

Fig.2 Dependence of the defect-density evolution on the impurity concentration C_M as a function of irradiation dose. Each symbol in the experimental data corresponds to an individual run.

Contact (Group Leader):

YAMASHITA Shinichiro

yamashita.shinichiro@jaea.go.jp

Research Group for High Temperature Science on Fuel Materials

We treat issues on nuclear fuel materials for both light water reactors (LWR) and advanced reactors in the future. Experimental works on uranium and non-radioactive materials are carried out in the Research building No. 4, with various heating devices and analytical apparatus. Those on transuranium elements (TRU: Pu and minor actinides) are performed at TRU-HITEC, consisting of specially designed hot cells and a glove box with a highly purified argon atmosphere. We also take advantage of computer science to understand or predict phenomena concerning the fuel materials at high temperatures and under the irradiation conditions.

FEMAXI Code and Nitride Fuel Property Database

Our tool to predict behavior of the transmutation fuels is the module for ADS (Accelerator Driven System) nitride fuel performance analysis, running on the computer code called FEMAXI. We have continuously improved the module for more reliability. Details of the current models and fuel materials properties in the module are described in the JAEA-Data/Code report[1].

For the practical analysis of the fuel behavior, the material property database developed with data on the actual fuel materials containing TRU is essential. The web version of our "Nitride Fuel Property Database" was opened in Oct. 2019 with a press release[2], and now any researchers can access it. Figure 1 shows the database interface. Users can see a graph as well as the data source and the function formula by choosing a composition of nitride.

Hot Experiments on TRU

To expand the database and the analysis module, we performed a series of annealing experiments on a (Pu,Cm,Zr)N nitride fuel pellet, in which Frenkel defects and He atoms accumulated due to alpha decay of ^{244}Cm for two years. Data on the dimensional recovery and the gas swelling caused by gaseous He release were successfully obtained as a function of temperature. These data will be reflected to the module with

apposite modelling. We also demonstrated the sintering of (Np,Zr)N pellets with applying pore former (organic polymer micro particles) to control the porosity (Figure 2). These hot experiments were carried out under the research project "R&D on nitride fuel cycle for MA transmutation to enhance safety and economy" funded by the MEXT.

Reference

1) H. Shibata et.al., Development of Module for ADS Nitride Fuel Performance Analysis, JAEA-Data/Code 2019-023, March 2020.
2) Press release, https://www.jaea.go.jp/english/news/press/2019/101801/ (accessed 2020-08-07)

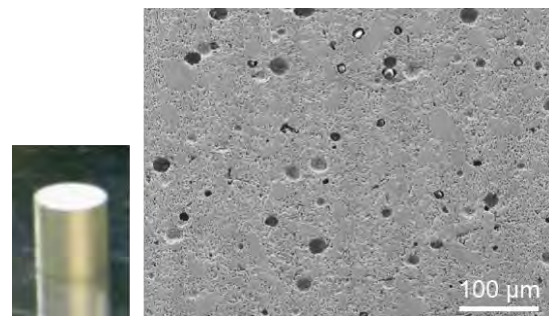**Fig.1 Example of the web database interface.**

Fig.2 Appearance of the sintered (Np,Zr)N pellet and the cross sectional image.

Contact (Group Leader):
TAKANO Masahide
takano.masahide@jaea.go.jp

Research Group for Radiochemistry

Radiochemistry provides fundamental information about the essential materials in developing nuclear technology by identification of the chemical reaction of radioactive materials by measurement and chemical separation. We chemically resolve various issues arisen from the nuclear industry by developing new technique of measurement and computational method.

Chemical Reactivity of Nuclear Fuel

Estimating the long-term degradation of fuel debris or the soundness of spent nuclear fuel in the geological repository requires basic understanding of redox reactions taking place at the surface of uranium (U) materials. Radiation-induced oxidative dissolution of uranium dioxide (UO_2) is one of the most important chemical processes of U driven by the redox reactions. Thus, we have investigated the effect of UO_2 stoichiometry on the oxidative dissolution of UO_2 induced by hydrogen peroxide (H_2O_2) and γ-ray irradiation, in order to understand the evolution of the reaction kinetics during the course of the surface oxidation[1].

By comparing the reaction kinetics of H_2O_2 between stoichiometric $UO_{2.0}$ and hyper-stoichiometric $UO_{2.3}$, we observed a significant difference in reaction rate and U dissolution kinetics. The stoichiometric $UO_{2.0}$ reacted with H_2O_2 much faster than the hyper-stoichiometric $UO_{2.3}$. The U dissolution from $UO_{2.0}$ was initially much lower than that from $UO_{2.3}$, but gradually increased as the surface oxidation by H_2O_2 proceeded (Figure 1). The γ-ray irradiation induced the U dissolution that is analogous to the kinetics by the exposure to a low concentration (0.2 mM) of H_2O_2. The exposure to higher H_2O_2 concentrations caused lower U dissolution and resulted in deviation from the U dissolution behavior driven by the water radiolysis.

Adsorption and Transfer of Radioactive Species on Solid Surface

Radioactive species in the environment transfer while repeating sorption and desorption on the surface of solid materials. Recently we have developed an optical microscopic technique to study the transfer of radioactive species on a solid surface, which requires a very small amount of a radioactive sample solution for the experiment[2]. In this study, an aqueous solution (0.5 μL) dissolving uranyl and europium ions was dropped on a dry silica gel plate to spread the two ions on the plate through the water flow caused by the capillary effect, and the distributions of the two ions adsorbed on the silica gel plate were separately measured using photoluminescence microspectroscopy. The photoluminescence images of uranium and europium (Figure 2) clearly show different distributions from each other, and uranium is distributed near the center whereas europium is distributed around the uranium distribution. The larger-area distribution of europium is caused because the uranyl ion is preferentially adsorbed to silica gel over the europium ion and the uranyl adsorption disturbs the adsorption of europium ion.

Reference

1) Y. Kumagai et al., Journal of Physical Chemistry C, 123, 9919-9925 (2019).
2) R. Kusaka et al., Journal of Nuclear Science and Technology, 57, 1046-1050 (2020).
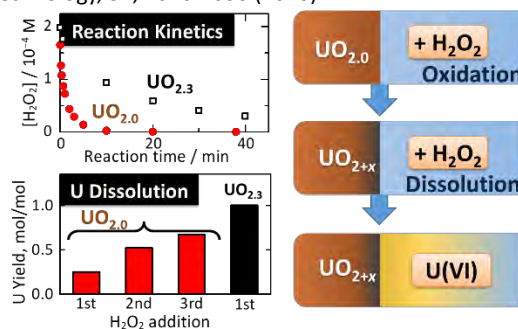
Fig.1 Change in the U dissolution kinetics due to the H_2O_2 oxidation of UO_2 (left) and schematic representation of the surface oxidation process (right).
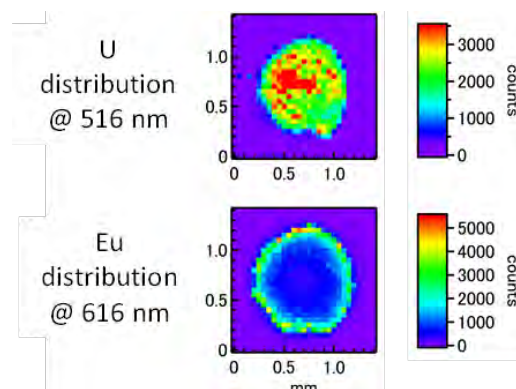
Fig.2 Photoluminescence images of uranium and europium distributions formed on a silica gel plate.

This figure is adapted by permission of Informa UK Limited, trading as Taylor & Francis Group, www.tandfonline.com on behalf of Atomic Energy Society of Japan. Application of photoluminescence microspectroscopy: a study on transfer of uranyl and europium ions on dry silica gel plate (Ref 2). Copyright 2020 © Atomic Energy Society of Japan.

Contact (Group Leader):
WATANABE Masayuki
watanabe.masayuki@jaea.go.jp

Research Group for Analytical Chemistry

Accurate analyses of radioactive substances are fundamental technologies supporting the nuclear technology. Control of the chemical state of the analyte and removal of interference elements prior to instrumental analysis are key techniques for the high precision chemical quantitative analysis. Speciation analysis is necessary to understand the behavior of radioactive elements such as actinides whose chemical properties differ depending on the species. Our group is developing practical analytical methods for actinide and fission products based on studies of elucidation of chemical reaction, ion separation phenomena such as adsorption, precipitation, aggregation, etc. It is engaged on instrumental analyses such as electrochemical method, microscopic analysis technology, etc.

In the decommissioning of the TEPCO Fukushima Daiichi Nuclear Power Plant (1F), there is concern about internal exposure due to ingestion of particulate matter containing alpha radionuclide into the body. Understanding their chemical properties is important for predicting those particulate formation and spreading behavior in contaminated workplaces.

Direct Quantitation Method Using Laser Ablation-ICP-MS

To reduce exposure during analysis of high radiation dose samples, simplified quantitation method for ^{135}Cs in the spent Cs adsorbent at 1F was developed[1]. It was examined that adsorbed Cs was directly measured by ICP-MS without elution and preparation of the solution sample. Crushing and subsequent coating with a nitrocellulose-based curing agent provided a thin flat surface and thus allowed for stable solid sampling during laser ablation. The use of the ^{135}Cs/^{137}Cs ratio measured by ICP-MS and ^{137}Cs radioactivity obtained by gamma spectrometry achieved simple and precise quantitation of ^{135}Cs, requiring only very small (<10 mg) samples.

Electrochemical Study of Formation of Actinide Colloidal Particles

Redox of actinide ions in weakly acidic solution is a complex reaction due to the formation of a precipitate. We tried to elucidate their reaction mechanism by electrochemical method and spectroscopy. Electric resistance of the electrode surface covered with uranium deposit exhibit a change in chemical form was studied by electrochemical impedance measurement and X-ray Absorption Fine Structure (XAFS). It was found that U deposits initially form low electrical resistance amorphous compound as intermediate, and they transfer to high electrical resistance crystalline compound while reaction rate depends on pH of the solution.

Speciation of α Radioactive Particles

Local speciation analysis for U in an alpha radioactive particle was tried based on micro Raman spectroscopy. To confirm its applicability to heterogeneous samples, Raman measurement of aged UO_2 particles was performed (Figure 1a). Mapping images with 1 μm width of Raman measurement were analyzed. Strong Raman shift of UO_2 at 1148 cm^{-1} was obtained in the whole particle (Figure 1b). Raman shift of uranium peroxide at 828 cm^{-1} was strongly observed locally (Figure 1c). By comparing the Raman spectrum measured at Spots A and B, it is possible to clearly identify UO_2 and uranium peroxide. Micro Raman mapping enables local speciation analysis with spatial resolution of 1 μm.

Reference

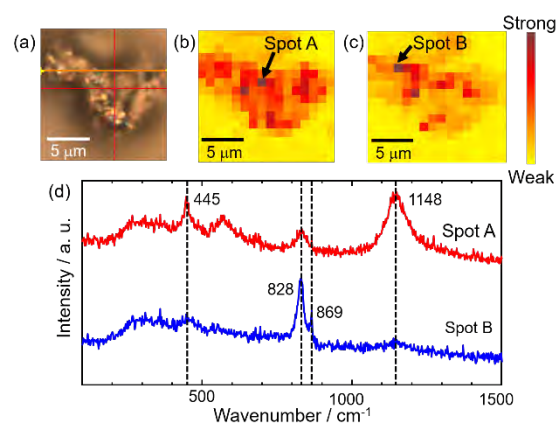1) S. Asai et al., Anal. Chem., 92, 3276 (2020).

Fig.1 Local speciation by Raman spectroscopy of aged UO_2 particle. (a) Optical microscope image, (b, c) Raman mapping images, (d) Raman shift at spots A and B.

Contact (Group Leader):
KITATSUJI Yoshihiro
kitatsuji.yoshihiro@jaea.go.jp

Research Group for Environmental Science

We are conducting research and development in order to upgrade the assessment technology of environmental radioactive materials, required for environmental impact assessment of various radionuclide releases and environmental pollution events. Computer models for simulations on the behavior of radioactive materials in the atmospheric, terrestrial, and oceanic environments are developed, and model validation and improvement are carried out using measured data around nuclear facilities. Environmental samples for model validation are obtained to evaluate temporal and spatial distributions of radionuclides, and the migration processes of radionuclides in the environment are elucidated by analysis of these data. Our technology has been applied to analyze the environmental behavior and impact of radioactive materials discharged due to the TEPCO Fukushima Daiichi Nuclear Power Plant (1F) accident.

Atmospheric Dispersion Simulation Regarding the 1F Accident

We carried out source term estimations and atmospheric dispersion simulations to evaluate the environmental impact caused by the 1F accident using the Worldwide version of System for Prediction of Environmental Emergency Dose Information (WSPEEDI). In the recent study, we further refined the source term estimated in our previous study and improved the atmospheric dispersion simulation with an optimization method using various measurements[1]. To apply this analysis to the local-scale atmospheric dispersion simulations, the new optimization method with combination of ensemble meteorological calculations and the Bayesian inference method was developed (Figure 1). This optimization improved not only the source term but also the wind field in meteorological calculations by selecting the optimum case from ensemble members of meteorological calculations based on comparison results between the dispersion calculations and measurements of radionuclides. As a result, the atmospheric dispersion simulation successfully reproduced both the air concentrations of ^{137}Cs and ^{131}I at monitoring points and their surface depositions measured by airborne monitoring (Figure 2). The deposition amount on the land decreased from 3.7×10^{15} Bq by the previous study to 2.1×10^{15} Bq, which was close to the measured amount of 2.4×10^{15} Bq.

We also constructed the database for spatiotemporal distribution of major radionuclides (total ^{131}I, ^{131}I chemical species (I$_2$, CH$_3$I, and particulate iodine), ^{134}Cs, ^{137}Cs, and ^{132}Te) in the air and on the surface by using the simulation results. This database was used for comprehensive dose assessment coupled with behavioral patterns of evacuees from the 1F accident by collaborating research groups in the Japanese dose assessment project[2]. The reproducibility of air concentration in our simulation became higher especially for the region of north of 1F. This area is important for dose estimation regarding the behavioral patterns of evacuees, and these improvements led to the refinement of dose estimation.
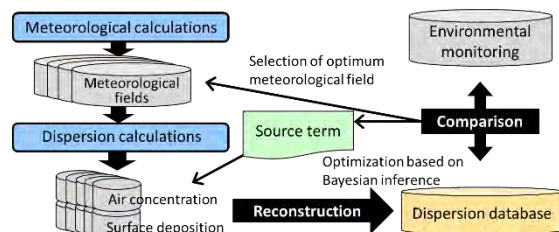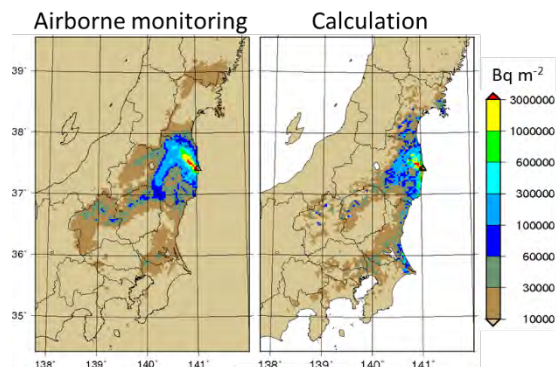
Fig.1 New optimization method

Fig.2 Deposition pattern of ^{137}Cs

Reference

1) H. Terada et.al., Journal of Environmental Radioactivity, 213, 106104, (2020).

2) T. Ohba et al., Scientific Reports, 10, 3639, (2020).

Contact (Group Leader):

NAGAI Haruyasu

nagai.haruyasu@jaea.go.jp

Research Group for Radiation Transport Analysis

Nowadays, a computer simulation technique that can analyze radiation transport in a material is an essential tool for research and development in the field of nuclear and radiation sciences. We have developed a radiation transport simulation code, the Particle and Heavy Ion Transport code System (PHITS), and apply it to industrial, scientific, and medical studies. PHITS has been upgraded to improve its reliability and to expand areas to be applied. In addition, we also conduct studies on radiological protection and radiation effects. Here, computational human models have been developed for dosimetry studies and an experiment has been carried out to study DNA damage from localized exposure to an insoluble cesium (Cs) particle.

Upgrade of PHITS

In FY2019, we released PHITS versions 3.17 and 3.20. The major upgraded features are as follows for these versions.

/ Proton (E < 300 MeV) and carbon ion (E < 10 MeV/n) track structure mode has been implemented in the recent versions of PHITS. A user can analyze points where ionization and excitation events might occur. This function is useful for studies on DNA damage, medical physics and so on.

/ A function has been implemented to read the stopping power of each material from the user-supplied table.

/ A function to read electro-magnetic field maps written in xyz or r-z grid has been implemented. This tool is useful for design of a beam line in an accelerator and so on.

/ We have improved DCHAIN that is used to calculate induced radioactivity. Several neutron activation libraries and decay-data libraries have been developed based on the latest evaluated nuclear data for DCHAIN. In addition, statistical uncertainties of the induced activities can be evaluated by DCHAIN. The new version of DCHAIN is called as DCHAIN-PHITS and included in the package of PHITS.

Please access PHITS home page[1], if you have an interest in further information on the code.

New Japanese Computational Models for Dosimetric Study

JAEA developed and has released Japanese adult computational models, JF-103 (female) and JM-103 (male). These models are constructed with the voxel (volume-pixel) format that consists of large number of cuboids with the size in mm-order. The

International Commission on Radiological Protection (ICRP) suggests new human models that are constructed with a format of tetrahedral structure. The new models can precisely depict skin and surface of small organs. So, we have developed new Japanese adult models with the new format. The posture can be easily changed in the new Japanese adult models (Figure 1). Thus, a user is to perform dosimetry study by taking account for an exposure condition. These models are to be released in the near future.

Fig.1 Japanese adult male computational model with the tetrahedral format in various postures

Experiment for DNA Damage during Exposure to an Insoluble Cs Particle

Insoluble Cs microparticles with radioactivity have been detected around the TEPCO Fukushima Daiichi Nuclear Power Plant after the accident in 2011. While a soluble Cs particle is distributed over a whole body, an insoluble Cs particle can remain in the respiratory system after inhalation. We have conducted experimental studies to investigate DNA damage in cultured cells from localized exposure by an insoluble Cs particle[2]. In addition, computational studies using PHITS were also performed to obtain dose distribution around cells where a Cs particle adheres. The results show that localized exposure to a Cs particle would give advantageous (repair) to proximal cells as well as disadvantageous (more damage) to distal cells.

Reference
1) PHITS home page, https://phits.jaea.go.jp/ (accessed 2020-08-04).
2) Y. Matsuya et al, Sci. Rep. 9-9483, (2019).

Contact (Group Leader):

TAKAHASHI Fumiaki

takahashi.fumiaki@jaea.go.jp

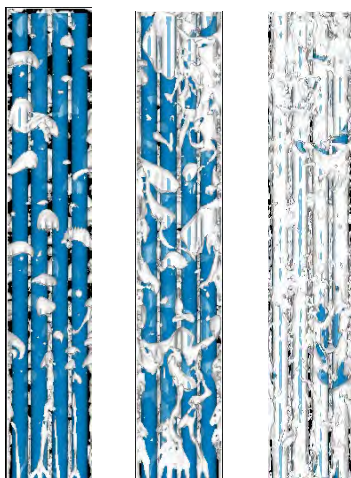# Development Group for Thermal-Hydraulics Technology

For the establishment of thermal-hydraulics numerical simulation methods for multi-phase flow, we are developing multi-phase CFD (computational fluid dynamics) numerical simulation codes for massive computers, TPFIT and JUPITER, measurement techniques to obtain detailed thermal-hydraulics data and performing thermal-hydraulics experiments to construct validation databases. These advanced techniques are applied to the research works for improving the safety of the LWRs and considering the decommissioning process of the TEPCO Fukushima Daiichi Nuclear Power Plant.

Multi-phase CFD codes

TPFIT is developed for two-phase flow in the nuclear reactor. TPFIT uses compressible fluid equations and can be applied to the numerical simulation of two-phase flow in any system.

JUPITER can simulate melting and relocation behavior without assumptions or simplification. A chemical reaction such as a eutectic reaction and oxidation model can also be taken into account. Besides, JUPITER can perform the massively parallel simulation of multi-phase flow with more than two hundred thousand cores, by adapting high-efficient parallel computing techniques.

As one of the examples of CFD codes, we performed a numerical simulation of two-phase flow in a 4×4 bundle of fuel rods by JUPITER (Figure 1)[1]. The diameter of the rods is 10 mm, and the pitch between the rods is 13 mm. In this simulation, superficial liquid velocity was 0.100 m/s, and superficial gas velocity was 0.034 (Case 1), 0.157 (Case 2), and 0.781 (Case 3) m/s. Based on existing knowledge, the interface shape of two-phase flow (so-called two-phase flow pattern) depends on superficial liquid and gas velocity[1], and numerical results reproduced this two-phase flow pattern.

TPFIT and JUPITER were released at PRODAS[2]. We are continuously improving TPFIT and JUPITER to enhance the safety of the LWRs.

Experimental Studies

We perform various experiments to validate those simulations and construct basic physical models. As one of the experiments, we performed optical measurement of aerosol particle capturing behavior near the gas-liquid interface (Figure 2)[3]. Aerosol particle capturing at the gas-liquid interface is utilized in water filtering industrially. The capturing is also used in the filtered venting systems and pool scrubbing in the nuclear reactor. We performed this experiment to understand the capturing mechanism and validate the numerical simulation results of TPFIT. By this experiment, we could visualize aerosol particle behavior. Based on the results, we concluded that an inertial impact of aerosol particles to a droplet occurs as one of the physical mechanisms of the aerosol particle capturing.
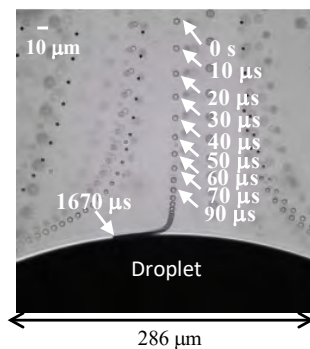
Fig.2 Composite image of continuous images particles near upper part of the droplet

References
1) A. Ono et al., Mechanical Eng. J. 7(3), 19-00583 (2019).
2) PRODAS (PROgram and DAtabase retrieval System), https://prodas.jaea.go.jp/ (accessed 2020-09-10)
3) S. Uesawa and H. Yoshida, et al., Proceedings of the 27th International Conference on Nuclear Engineering (ICONE-27), ICONE27-1972 (2019).

Contact (Group Leader):
YOSHIDA Hiroyuki
yoshida.hiroyuki@jaea.go.jp

(a) Case 1   (b) Case 2   (c) Case 3

Fig.1 Numerical simulation of two-phase flow in 4×4 bundle

Development Group for LWR Advanced Technology

This group was founded to conduct a research program to improve light water reactor (LWR) safety from a scientific point of view. Through this, the group wants to contribute to the advance of the safety technology in LWR, and also accelerates the decommissioning and dismantling of the TEPCO Fukushima Daiichi Nuclear Power Plant (1F).

This group mainly conducts studies on fission product (FP) behaviors under normal and accident conditions and development of accident tolerant fuel (ATF) cladding.

Fission Product Behavior

We are constructing a database of FP chemistry named ECUME (Effective Chemistry database of fission products Under Multiphase rEaction)[1]. ECUME covers important phenomena revealed after the 1F severe accident (SA). According to TEPCO's report of the investigation in the internal of primary containment vessel (PCV) of 1F unit 2[2], the measured dose rate was 10 Gy/h at the pedestal area, where most debris should exist, while it was 70-80 Gy/h in the vicinity. It was reported that deposits were found in this vicinity, and these can be believed as the source of higher dose rate. From the information of condition and location, we assumed that the suspected materials for the deposits were the thermal insulation (i.e. calsil) which covers the main steam piping. We presumed that steam containing FPs such as Cs was leaked from safety relief valves and blew off the calsil which was adsorbing Cs. Therefore, as an initial step, we investigated interaction temperature between the calsil and Cs with effect of atmospheres. As the results, it was suggested that some chemical interaction between calsil and Cs (i.e. CsOH) occurred in the temperature range of 575-730°C, regardless of Ar-5%H_2 and Ar-20%H_2O atmospheres. Furthermore, the X-ray diffraction (XRD) analyses have indicated that cesium aluminum silicate, $CsAlSiO_4$ was formed in the test (Figure 1)[3]. Aluminum was present as an impurity or adduct in the calsil.

Accident Tolerant Fuel (ATF)[*]

For further improvement of safety of the existing LWRs, ATFs are being developed. In Japanese development program, FeCrAl-ODS steel for boiling water reactor (BWR) and SiC fiber reinforced SiC matrix composite (SiC/SiC) for BWR and pressurized water reactor (PWR) were selected as major ATF cladding concepts. Out of pile tests with the SiC/SiC composite tubes were performed to investigate the behavior in loss of coolant accident (LOCA). The test rod consisted of the SiC/SiC cladding and alumina insert. The upper end of the test rod was connected to a load cell. The lower end was connected to an argon pressurizer to control internal pressure of the test rod. The connected parts were sealed with epoxy. The test rod was pressurized with argon gas up to 7 MPa. The test chamber was filled with steam, and the test rod was heated up to the peak temperature of 1200°C by 5°C/sec. The test rod was kept at the peak temperature for the holding time of 100 sec. The equivalent cladding reacted (ECR) to the peak temperature of 1200°C and the holding time of 100 sec was 15%. The heater was turned off and simultaneously the water was fed from the water feeder at the bottom of the test chamber. When the test rod was quenched, the axial force of 540 N was applied to the test rod. The test rod did not fail beyond the conditions corresponding to the current LOCA criteria. It was demonstrated that SiC/SiC cladding could keep fuel pellet inside the cladding even in beyond design-basis-accident condition. After the above integral LOCA test, the test rod was subjected to the axial tensile test at room temperature. There was no difference in maximum load between before and after the integral LOCA tests. This indicates that the mechanical strength of the SiC cladding was not degraded by severe thermal and mechanical load under the LOCA condition[4].
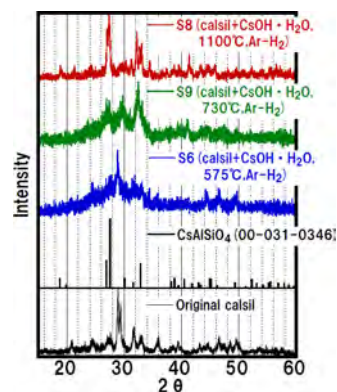
Fig.1 XRD patterns of calsil mixed with $CsOH \cdot H_2O$ in Ar-5%H_2

References
1) Development Group for LWR Advanced technology, JAEA-Data/code 2019-017 (2020).
2) Tokyo Electric Power Company, The 5th Progress Report on 1F Accident, Attachment 4 (2017).
3) M. Rizaal et al., J. Nucl. Sci. Technol., to be in press.
4) K.Furumoto et al., Proc of TOPFUEL2019, (2019) 830-835.

Contact (Group Leader):
NEMOTO Yoshiyuki
nemoto.yoshiyuki@jaea.go.jp

Research Group for Partitioning

Partitioning and transmutation has been proposed as a strategy for managing high-level radioactive waste (HLW) generated by reprocessing of spent nuclear fuels via a hydrometallurgical method. HLW consists of many elements of different radiotoxicities and chemical properties. Thus, it is reasonable to separate the elements into groups instead of treating them together from the viewpoint of increasing transmutation efficiency and reducing disposal area.

To this end, our research group has been developing several extractants and has investigated their extraction properties. Recently, we proposed a novel hydrometallurgical process called SELECT (Solvent Extraction from Liquid waste using Extractants of CHON-type for Transmutation) to recycle nuclear materials and separate actinides for transmutation[1].

A Demonstration Test of SELECT in a Hot-Cell

A conceptual flow sheet of SELECT process is shown in Figure 1. This process consists of the following four steps: (i) recovery of U and Pu from dissolution solution of spent nuclear fuels, (ii) recovery of Am, Cm, and rare earth elements (REs) from HLW, (iii) separation of Am and Cm from REs, and (iv) separation of Am and Cm. The extractants used in this process consist of carbon, hydrogen, oxygen, and nitrogen, and thus can be decomposed into gases by incineration. This contributes to reducing the volume of secondary solid waste.

We carried out continuous counter-current experiments for steps (i) and (ii), and demonstrated the validity of each step. For further development of SELECT process, a continuous counter-current experiment for step (iii) was performed using HONTA as an extractant with mixer-settler extractors installed in a hot-cell (Figure 2) at NUCEF (NUclear fuel Cycle safety Engineering research Facility). A nitric acid containing Am, Cm, and REs obtained by an experiment for step (ii) was used as the feed. The experiment was conducted over a cumulative operation time of 14 h. HONTA diluted with n-dodecane extracted Am and Cm in the feed. The recoveries of Am and Cm were 94.9% and 78.9%, respectively, and these values were similar to the predicted ones obtained by a simulation code called PARC[2,3]. PARC indicated that the recoveries could be ≥99% by optimizing separation conditions such as nitric acid concentration and flow rate. These results support the applicability of HONTA as an extractant to separate Am and Cm from REs.

In addition to developing separation process with novel extractants, other studies, such as to evaluate radiolysis of the extractants and to improve the PARC code, have been carried out.
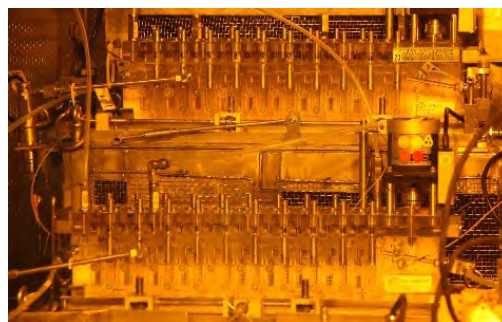
Fig. 2 Mixer-settler extractors used in the continuous counter-current experiment

Reference
1) Y. Ban et al., Solvent Extra. Ion Exch., **37**, 27-37, (2019).
2) Y. Ban et al., Solvent Extra. Ion Exch., **37**, 489-499, (2019).
3) Y. Tsubata et al., JAEA-Data/Code, 2008-010, (2008).

Contact (Group Leader):

BAN Yasutoshi

ban.yasutoshi@jaea.go.jp

Fig. 1 A conceptual flow sheet of SELECT process and proposed extractants in each step

Research Group for Nuclear Transmutation System

Research Group for Nuclear Transmutation System is developing Accelerator Driven System (ADS) devoted to transmutation of Minor Actinide (MA) into short-lived or stable nuclide. Present R&D level on ADS is at maturing of conceptual design and testing by small-scale equipment for each component and material. To improve ADS design, we are developing analysis systems consisting of particle transport, thermal-hydraulics, material, and plant behavior. Moreover, we are developing sub-critical monitoring techniques for safe and effective operation of ADS.

New Method for Sub-Criticality Measurement

Accurate sub-criticality measurement is a key issue for operation of ADS whose core must be at a sub-critical state. The pulsed neutron source (PNS) method is one of the promising sub-criticality measurement techniques. In this method, the sub-criticality is estimated by measuring decay constants of neutron counts after each pulse injection of proton beam which generates spallation neutrons at the center of the core. The problem of this method is that the decay constants are affected by detector positions and it can impose an error on the sub-criticality measurement. For example, neutron counts of a detector near the generation point of spallation neutrons seemingly decay more rapidly than that in the peripheral position because neutrons produced by proton beam directly enter the detector without fissions. The conventional PNS method mitigates this error by ignoring some of the neutron counts right after the proton injection, but the error due to spatial dependence still remains.

To overcome this problem, a new method, the linear combination method (LCM), has been proposed, which aims to mitigate the spatial dependence by linear combination of neutron counts obtained at multiple detectors [1] and provides one unique estimation of sub-criticality. It essentially reduces the error by the detector position. Figure 1 shows an experimental result conducted at Kyoto University Critical Assembly (KUCA). Figure 2 shows the core configuration of the experiment. The result of the decay constant by LCM has less dependence on the masking time (range of ignored counts) while the results by the conventional method depend on both detector position and the masking time.

Reference
1) R. Katano, Nuclear Science and Engineering 193 (4), p. 431-439, (2019).
2) R. Katano et al., Nuclear Science and Engineering 193 (12), p. 1394-1402, (2019).

Contact (Group Leader):

NISHIHARA Kenji

nishihara.kenji@jaea.go.jp

Fig. 1 Results of the PNS experiment at KUCA [2]

Fig. 2 Core configuration of KUCA

Neutron counts from 5 detectors decay after proton pulse injection (top left). By the conventional method, neutron counts are converted to decay constant unique to the ADS, but it problematically depends on detector position and masking time (top right). In the new LCM method, 5 neutron counts are combined to one neutron counts (bottom left) and a unique decay constant with less effect of masking time is obtained (bottom right)

Research Group for MA Transmutation Fuel Cycle

Feasibility study on transmutation system shows that only 20 % of minor actinides (MAs) in the fuels can be transmuted in one burning cycle of about 2 years. Reprocessing of the spent fuels is necessary to transmute MAs remaining in the spent fuels. Repeating fuel fabrication, transmutation, and reprocessing can transmute most of MAs coming to the dedicated MA transmutation fuel cycle in the double-strata fuel cycle concept. We have been carrying out research and development of the technology on reprocessing of spent MA transmutation fuels. One of our concerns is on pyroprocessing technology, in which molten salts and liquid metals are used as solvents; this technique is suitable for reprocessing spent MA nitride fuels.

Material Balance Calculation on the Electrorefining Process

We have proposed a flowsheet for the electrorefining process of spent MA nitride fuels, based on that designed for metal fuel treatment. The flowsheet contains the salt recycling process to control the contamination of fission products (FPs) in the MAs recovered by electrorefining. FPs are constantly removed from the molten salt bath via this process, which includes multistage reductive extraction of actinides using molten salt/liquid Cd phases and zeolite treatment to absorb FP by ion exchange or occlusion of FP chlorides. The salt-loaded zeolite is to be immobilized in glass-bonded sodalite for disposal in a geological repository.

Material balance calculation is useful to quantify the scale of equipment needed to achieve the desired outputs of the process and to examine the impact of processing conditions. Such attempts were made on the electrorefining process of spent MA transmutation nitride fuels for the accelerator-driven system (ADS). The conditions of the process are needed to meet the target recovery yield of MA (99.9 %) and the acceptable impurity level of rare earths (REs) fission products in the recovered material (RE/MA < 5 wt.%).

We examined the impact of the conditions in the salt recycling process such as stage numbers of the countercurrent reductive extraction and the zeolite treatment on material balance including quantity of the secondary wastes. Table 1 shows the conditions of the calculations. The composition of the spent MA nitride fuel was determined by the latest burn-up calculation for the initial fuel containing 5 wt.% RE against MA. Distribution of the elements in each step was calculated based on the experimental data in literature. Table 2 shows the conditions of the process and the amounts of the glass-bonded sodalite waste. The results show that multistage reductive extraction treatment is necessary to meet the targets, and the amount of the salt transferred to the recycling process per day is only 2-3 % of the molten salt bath. On the other hand, the stage number of the zeolite treatment is recommended to be more than three from the aspect of quantity of glass-bonded sodalite wastes [1].

Table 1 Conditions of the electrorefining process.

Number of ADS	1
Spent MA nitride fuel/ ADS・cycle	7789 kg
Actinides in spent fuel/ ADS・cycle	4217 kg
Number of electrorefiner	1
Molten salt in electrorefiner	1000 kg
Actinides content in molten salt	6 wt.%
Liquid Cd cathode in electrorefiner	200 kg
Operating days	200

Table 2 The effect of the stage numbers for each step on quantity of the glass-bonded sodalite waste.

Stage number		Salt transferred to the recycling process (kg/day)	Glass-bonded sodalite waste (kg/fuel cycle)
reductive extraction	zeolite treatment		
1	3	-	-
2	3	32	6680
3	3	22	5790
4	3	20	5660
5	3	19	5610
3	2	22	8040
3	4	22	5480
2	2	32	10020
2	4	32	5870

Reference

1) H. Tateno, T. Sato, Y. Tsubata, H. Hayashi, J. Nucl. Sci. Technol., 57(3) 224-235 (2020).

Contact (Group Leader):

HAYASHI Hirokazu

hayashi.hirokazu55@jaea.go.jp

Publication list

Nuclear Data and Reactor Engineering Division

Nuclear Data Center

Papers

1) Consistent description of light composite particle emission in deuteron-induced reactions, S. Nakayama, O. Iwamoto & Y. Watanabe, *Phys. Rev. C* 100(4), 044603 (2019).

2) Spin-isospin properties of *N = Z* odd-odd nuclei from a core+*pn* three-body model including core excitations, F. Minato & Y. Tanimura, *Eur. Phys. J. A* 56, 45 (2020).

3) Measurements of the Am-243 neutron capture and total cross sections with ANNRI at J-PARC, A. Kimura, S. Nakamura, K. Terada, T. Nakao, K. Mizuyama, N. Iwamoto, O. Iwamoto, H. Harada, T. Katabuchi, M. Igashira, T. Sano, Y. Takahashi, C.H. Pyeon, S. Fukutani, T. Fujii, T. Yagi, K. Takamiya & J.-I. Hori, *J. Nucl. Sci. Tech.* 56(6), 479 (2019).

4) Measurements of thermal-neutron capture cross -section and resonance integral of neptunium-237, S. Nakamura, F. Kitatani, A. Kimura, A. Uehara & T. Fujii, *J. Nucl. Sci. Tech.* 56(6), 493 (2019).

5) Measurements of thermal-neutron capture cross -section of Cesium-135 by applying mass spectrometry, S. Nakamura, Y. Shibahara, A. Kimura, O. Iwamoto, A. Uehara & T. Fujii, *J. Nucl. Sci. Tech.* 57(4), 388 (2020).

6) Phenomenological level density model with hybrid parameterization of deformed and spherical state densities, N. Furutachi, F. Minato & O. Iwamoto, *J. Nucl. Sci. Tech.* 56(5), 412 (2019).

7) Statistical properties of thermal neutron capture cross sections calculated with randomly generated resonance parameters, N. Furutachi, F. Minato & O. Iwamoto, *Phys. Rev. C* 100(1), 014610 (2019).

8) JENDL/ImPACT-2018: a new nuclear data library for innovative studies on transmutation of long-lived fission products, S. Kunieda, N. Furutachi, F. Minato, N. Iwamoto, O. Iwamoto, S. Nakayama, S. Ebata, T. Yoshida, K. Nishihara, Y. Watanabe & K. Niita, *J. Nucl. Sci. Tech.* 56(12), 1073 (2019).

9) Reference database for photon strength functions, S. Goriely, P. Dimitriou, M. Wiedeking, T. Belgya, R. Firestone, J. Kopecky, M. Krtička, V. Plujko, R. Schwengner, S. Siem, H. Utsunomiya, S. Hilaire, S. Péru, Y.S. Cho, D.M. Filipescu, N. Iwamoto, T. Kawano, V. Varlamov & R. Xu, *Eur. Phys. J. A* 55, 172 (2019).

10) Neutron capture cross-section measurement and resolved resonance analysis of Np-237, G. Rovira, T. Katabuchi, K. Tosaka, S. Matsuura, K. Terada, O. Iwamoto, A. Kimura, S. Nakamura, N. Iwamoto, M. Segawa & M. Maeda, *J. Nucl. Sci. Tech.* 57(1), 24 (2020).

11) IAEA photonuclear data library 2019, T. Kawano, Y.S. Cho, P. Dimitriou, D. Filipescu, N. Iwamoto, V. Plujko, X. Tao, H. Utsunomiya, V. Varlamov, R. Xu, R. Capote, I. Gheorghe, O. Gorbachenko, Y.L. Jin, T. Renstrøm, M. Sin, K. Stopani, Y. Tian, G.M. Tveten, J.M. Wang, T. Belgya, R. Firestone, S. Goriely, J. Kopecky, M.Krtička, R. Schwengner, S. Siem & M. Wiedeking, *Nucl. Data Sheets* 163, 109 (2020).

12) Enhancement of element production by incomplete fusion reaction with weakly bound deuteron, H. Wang, H. Otsu, N. Chiga, S. Kawase, S. Takeuchi, T. Sumikama, S. Koyama, H. Sakurai, Y. Watanabe, S. Nakayama, D.S. Ahn, H. Baba, S.D. Chen, K. Chikaato, M.L. Cortés, N. Fukuda, A. Hirayama, R. Hosoda, T. Isobe, S. Kawakami, Y. Kondo, S. Kubono, Y. Maeda, S. Masuoka, S. Michimasa, I. Murray, R. Nakajima, T. Nakamura, K. Nakano, M. Nishimura, T. Ozaki, A. Saito, T. Saito, H. Sato, Y. Shimizu, S. Shimoura, P.-A. Söderström, Y. Soudo, X.H. Sun, J. Suwa, D. Suzuki, H. Suzuki, H. Takeda, M. Takechi, Y. Togano, T. Tomai, H. Yamada, M. Yasuda & K. Yoshida, *Communications Phys.* 2, 78 (2019).

13) Conceptual study on parasitic low-energy RI beam production with in-flight separator BigRIPS and the first stopping examination for high-energy RI beams in the parasitic gas cell, T.

Sonoda, I. Katayama, M. Wada, H. Iimura, V. Sonnenschein, S. Iimura, A. Takamine, M. Rosenbusch, T.M. Kojima, D.S. Ahn, N. Fukuda, T. Kubo, S. Nishimura, Y. Shimizu, H. Suzuki, H. Takeda, M. Tanigaki, H. Tomita, K. Yoshida & H. Ishiyama, *Prog. Theor. Exp. Phys.* 2019(11), 113D02 (2019).

14) Anomalous radioisotope production for ^{68}ZnO using polyethylene by accelerator neutrons, K. Tsukada, Y. Nagai, S. Hashimoto, F. Minato, M. Kawabata, Y. Hatsukawa, K. Hashimoto, S. Watanabe, H. Saeki & S. Motoishi, *J. the Phys. Soc. Jpn* 89(3), 034201 (2020).

15) Measurement of the ^{235}U(n,f) cross section relative to the ^{6}Li(n,t) and ^{10}B(n,α) standards from thermal to 170 keV neutron energy range at n_TOF, S. Amaducci, *et al.* (The n_TOF Collaboration (H. Harada & A. Kimura)), *Eur. Phys. J. A* 55, 120 (2019).

16) Measurement of the ^{70}Ge(n,γ) cross section up to 300 keV at the CERN n_TOF facility, A. Gawlik, *et al.* (The n_TOF Collaboration (H. Harada & A. Kimura)), *Phys. Rev. C* 100(4), 045804 (2019).

17) Fission program at n_TOF, L. Tassan-Got, *et al.* (The n_TOF Collaboration (A. Kimura)), *EPJ Web of Conf.* 211, 03006 (2019).

18) PR10-7 activation measurement for thermal-neutron capture cross-section of Cesium-135, S. Nakamura, A. Kimura, O. Iwamoto, Y. Shibahara, A. Uehara & T. Fujii, *KURNS PROGRESS REPORT 2018*, 106 (2019).

19) Diagnostic (^{99}Mo/^{99m}Tc) and therapeutic (^{67}Cu) radioisotopes produced by neutrons from C,Be(d,n), Y. Nagai, K. Hashimoto, M. Kawabata, K. Tsukada, Y. Hatsukawa, F. Minato, Y. Sugo, H. Saeki, Si. Motoishi, *CERN Proc.* 1 *(Proc. the 15th Int. Conf. on Nucl. Reaction Mechanism)*, 333 (2019).

JAEA Reports

1) Status and future plan of JENDL, O. Iwamoto, *JAEA-Conf 2019-001 (Proc. the 2018 Symposium on Nuclear Data November 29-30, 2018, Tokyo Institute of Technology, Ookayama Campus, Tokyo, Japan)*, 7 (2019).

2) Gamow-teller strength distribution of nickel isotopes with odd number of neutron, F. Minato, *JAEA-Conf 2019-001 (Proc. the 2018 Symposium on Nuclear Data November 29-30, 2018, Tokyo Institute of Technology, Ookayama Campus, Tokyo, Japan)*, 173 (2019).

3) Measurement of the neutron capture cross section of ^{237}Np using ANNRI at MLF/J-PARC, G. Rovira, T. Katabuchi, K. Tosaka, S. Matsuura, K. Terada, O. Iwamoto, A. Kimura, S. Nakamura & N. Iwamoto, *JAEA-Conf 2019-001 (Proc. the 2018*

Symposium on Nuclear Data November 29-30, 2018, Tokyo Institute of Technology, Ookayama Campus, Tokyo, Japan), 83 (2019).

4) Neutron capture reaction data measurement of minor actinides in fast neutron energy region for study on nuclear transmutation system, T. Katabuchi, O. Iwamoto, J. Hori, N. Iwamoto, A. Kimura, S. Nakamura, Y. Shibahara & K. Terada, *JAEA-Conf 2019-001 (Proc. the 2018 Symposium on Nuclear Data November 29-30, 2018, Tokyo Institute of Technology, Ookayama Campus, Tokyo, Japan)*, 193 (2019).

5) Survey of computational methods of cross sections for thermal neutron scattering by liquids, A. Ichihara, *JAEA-Review 2019-046* (2020).

Research Group for Reactor Physics and Standard Nuclear Code System

Papers

1) Development of a handy criticality analysis tool for fuel debris, K. Tada, *Proc. ICONE27*, 1151 (2019).

2) Investigation of the impact of the prediction error of the burn-up code system SWAT4.0 on neutronics calculation, K. Tada & T. Sakino, *Proc. ICNC 2019 (11th International Conference on Nuclear Criticality safety)* (2019).

3) Treatment of R-matrix limited formula in FRENDY, K. Tada & S. Kunieda, *Proc. RPHA19 (Reactor PHysics Asia 2019)*, 229 (2019).

4) Implementation of random sampling for ACE

format cross sections using FRENDY and application to uncertainty reduction, R. Kondo, T. Endo, A. Yamamoto & K. Tada, *Proc. M&C 2019* (2019).

5) TENDL-2017 benchmark test with iron shielding experiment at QST/TIARA, S. Kwon, C. Konno, M. Ohta, K. Ochiai, S. Sato & A. Kasugai, *Fusion Eng. Design* 144, 209 (2019).

6) Problems of DPA cross-sections above 20 MeV in FENDL-3.1d found in A-FNS neutronics analysis, S. Kwon, C. Konno, M. Ohta & A. Kasugai, *J. Nucl. Sci. Tech.* 57(3), 344 (2020).

7) IRDFF-II: A new neutron metrology library, A. Trkov, P.J. Griffin, S.P.Simakov, L.R.Greenwood, K.I. Zolotarev, R. Capote, D.L. Aldama, V. Chechev, C. Destouches, A.C. Kahler, <u>C. Konno</u>, M. Koštál, M. Majerle, E. Malambu, M. Ohta, V.G. Pronyaev, V. Radulović, S. Sato, M. Schulc, E. Šimečková, I. Vavtar, J. Wagemans, M. White & H. Yashima, *Nucl. Data Sheets* 163, 1 (2020).

8) FRENDY Nuclear data processing system, <u>K. Tada</u>, *Nuclear Data Newsletter* 67, 2 (2019).

JAEA Reports

1) Nuclear data processing code FRENDY, <u>K. Tada</u>, *JAEA-Conf 2019-001 (Proc. the 2018 Symposium on Nuclear Data November 29-30, 2018, Tokyo Institute of Technology, Ookayama Campus, Tokyo, Japan)*, 29 (2019).

2) Problems of TENDL-2015 official ACE files, <u>C. Konno</u> & S. Kwon, *JAEA-Conf 2019-001 (Proc. the 2018 Symposium on Nuclear Data November 29-30, 2018, Tokyo Institute of Technology, Ookayama Campus, Tokyo, Japan)*, 167 (2019).

3) Development of Inventory Calculation Modules using ORIGEN-S for Decommissioning, <u>N. Matsuda</u>, C. Konno, T. Ikehara, K. Okumura & K. Suyama, *JAEA-Data/Code 2020-003* (2020) (*in Japanese*).

Research Group for Nuclear Sensing

Papers

1) Performance of large volume scintillation detector equipped with specially-designed shield for neutron resonance capture analysis, <u>H. Tsuchiya</u>, M. Koizumi, F. Kitatani & H. Harada, *Nucl. Inst. & Methods in Phys. Res., A* 932, 16 (2019).

2) Conceptual study on a novel method for detecting nuclear material using a neutron source, <u>M. Komeda</u> & Y. Toh, *Annals Nucl. Energy* 135, 106993 (2020).

3) Simulation study on the design of nondestructive measurement system using fast neutron direct interrogation method to nuclear materials in fuel debris, <u>M. Maeda</u>, K. Furutaka, M. Kureta, A. Ohzu, M. Komeda & Y. Toh, *J. Nucl. Sci. Tech.* 56(7), 617 (2019).

4) Non-destructive analysis of samples with a complex geometry by NRTA, <u>F. Ma</u>, S. Kopecky, G. Alaerts, H. Harada, J. Heyse, F. Kitatani, G. Noguere, C. Paradela, L. Šalamon, P. Schillebeeckx, H. Tsuchiya & R. Wynants, *J. Anal. At. Spectrom.* 35(3), 478 (2020).

5) Gamma-ray glow preceding downward terrestrial gamma-ray flash, Y. Wada, T. Enoto, Y. Nakamura, Y. Furuta, T. Yuasa, K. Nakazawa, T. Morimoto, M. Sato, T. Matsumoto, D. Yonetoku, T. Sawano, H. Sakai, M. Kamogawa, T. Ushio, K. Makishima & <u>H. Tsuchiya</u>, *Communications Phys.* 2, 67 (2019).

6) Downward terrestrial gamma-Ray flash observed in a winter thunderstorm, Y. Wada, T. Enoto, K. Nakazawa, Y. Furuta, T. Yuasa, Y. Nakamura, T. Morimoto, T. Matsumoto, K. Makishima & <u>H. Tsuchiya</u>, *Phys. Rev. Lett.* 123(6), 061103 (2019).

7) Neutron capture cross-section measurement and resolved resonance analysis of Np-237, G. Rovira, T. Katabuchi, K. Tosaka, S. Matsuura, K. Terada, O. Iwamoto, A. Kimura, S. Nakamura, N. Iwamoto, <u>M. Segawa</u> & M. Maeda, *J. Nucl. Sci. Tech.* 57(1), 24 (2020).

8) Feasibility study of two-dimensional neutron-resonance thermometry using molybdenum in 316 stainless-steel, T. Kai, K. Hiroi, Y. Su, <u>M. Segawa</u>, T. Shinohara, Y. Matsumoto, J.D. Parker, H. Hayashida & K. Oikawa, *Mater. Res. Proc.* 15(Neutron Radiography - WCNR-11), 149 (2020).

9) Development of active neutron NDA System for radioactive nuclear materials, <u>F. Kitatani</u>, H. Tsuchiya, A. Ohzu, M. Komeda, K. Furutaka, M. Maeda & Y. Toh, *Proc. INMM-60* (2018).

10) Performance evaluation of differential die-away system in an integrated active neutron NDA system for nuclear non-proliferation and nuclear security, <u>A. Ohzu</u>, M. Maeda, M. Komeda & Y. Toh, *Conf. Record 2018 IEEE NSS/MIC* (2019).

11) On-site measurement of nuclear material by using the fast neutron direct interrogation method, <u>M. Komeda</u>, ぶんせき *Bunseki* 2019(10), 459 (2019) (*in Japanese*).

12) Gamma-ray observations at the coastal area of Japan Sea in winter seasons, <u>H. Tsuchiya</u>, T. Enoto, Y. Wada, Y. Furuta, K. Nakazawa, T. Yuasa, D. Umemoto, K. Makishimai, & the GROWTH collaboration, *Proc. ICRC2019 (36th Int. Cosmic Ray Conf.)* (2019).

13) Sample shape effect on nuclear material

quantification with neutron resonance transmission analysis, <u>H. Tsuchiya</u>, F. Ma, F. Kitatani, C. Paradella, J. Heyse, S. Kopecky & P. Schillebeeckx, *Proc. 41st ESARDA Annual Meeting*, 374 (2019).

JAEA Report

1) Development of active neutron NDA system, <u>Y. Toh</u>, *JAEA-Conf 2019-001 (Proc. the 2018 Symposium on Nuclear Data November 29-30,*

14) High-energy atmospheric phenomena initiated by lightning, T. Enoto, Y. Wada & <u>H. Tsuchiya</u>, 日本物理学会誌 *Butsuri* 74(4), 192 (2019) (*in Japanese*).

2018, Tokyo Institute of Technology, Ookayama Campus, Tokyo, Japan), 47 (2019).

Patents

1) <u>Segawa M.</u>, Maeda M., Toh Y. & Kai T., "Method and system for measuring temperature", *Japanese Patent Application* 2019-100962 (2019.05.30)
2) <u>Segawa M.</u>, Toh Y., Maeda M. & Nishinaka I., "Method and system for analyzing alpha-ray

emitting nuclides", *Japanese Patent Application* 2019-136227 (2019.07.24)
3) <u>Komeda M.</u> & Toh Y., "Nuclear material detection device, Nuclear material detection method, Sample analysis method", *Japanese Patent Application* 2020-006793 (2020.01.20)

Fuels and Materials Engineering Division

Research Group for Corrosion Resistant Materials

Papers

1) Analysis for the mechanism of accelerated corrosion on low alloy steel in air-solution alternating condition, <u>K. Otani</u>, T. Tsukada & F. Ueno, 材料と環境 *Zairyo-to-Kankyo* 68(8), 205 (2019) (*in Japanese*)
2) Modelling of intergranular corrosion using cellular automata-II Numerical calculation results and comparison of intergranular

corrosion of stainless steels using cellular automata, <u>T. Igarashi</u>, E. Irisawa, A. Komatsu, M. Yamamoto & F. Ueno, *Proc. EUROCORR 2019*, 186704 (2019).
3) The accelerated corrosion of carbon steel in air-solution alternating condition, <u>K. Otani</u>, T. Tsukada, H. Terakado, K. Ebata & F. Ueno, *Proc. EUROCORR 2019*, 176540 (2019).

Patent

1) Ueda M., Hayashi Y., Kawamura K., <u>Irisawa E.</u>, <u>Komatsu A.</u>, Okubo N., *et al.*, "Metal oxide thin

film reduction sensor", *Japanese Patent Application* 2020-0062404 (2020.03.31)

Research Group for Radiation Materials Engineering

Papers

1) Alloy design for improvement of ductility and toughness in magnesium alloy; First-principles-calculation approaches, <u>T. Tsuru</u>, *J. Jpn Inst. Light Metals* 70(2), 73 (2020) (*in Japanese*).
2) Effects of one-dimensional migration of self-interstitial atom clusters on the decreasing behaviour of their number density in electron-irradiated α-iron, <u>Y. Abe</u>, Y. Satoh, N. Hashimoto & S. Ohnuki, *Philosophical Magazine* 100(1), 110

(2020).
3) Influence of long-term thermal aging on SCC initiation susceptibility of L-grade austenitic stainless steel, <u>K. Kondo</u>, S. Aoki, Y. Fujimura, T. Hirade, Y. Kaji & S. Yamashita, *Proc. 2019 Environ. Degradation of Mater. in Nucl. Power Systems-Water Reactors* (2019).
4) Stability of γ' precipitates in nickel based oxide dispersion-strengthened superalloys under high-

temperature and heavy irradiation Conditions, A. Konno, N.H. Oono, S. Ukai, S. Kondo, O. Hashitomi & A. Kimura, *Mater. Trans.* 60(11), 2260 (2019).

5) FE-SEM observations of multiple nanohillocks on $SrTiO_3$ irradiated with swift heavy ions, A. Kitamura, N. Ishikawa, K. Kondo, Y. Fujimura, S. Yamamoto & T. Yamaki, *Trans. The Mater. Res. Soc. Jpn* 44(3), 85 (2019).

6) Control of the size of etchable ion tracks in PVDF – Irradiation in an oxygen atmosphere and with fullerene C_{60}, A. Kitamura, T. Yamaki, Y. Yuri, H. Koshikawa, S.-i. Sawada, T. Yuyama, A. Usui & A. Chiba, *Nucl. Inst. & Methods in Phys. Res., B* 460, 254 (2019).

7) Anomalous solution softening by unique energy balance mediated by kink mechanism in tungsten-rhenium alloys, T. Tsuru, M. Wakeda, T. Suzudo, M. Itakura & S. Ogata, *J. Applied Phys.* 127, 025101 (2020).

8) Positronium in room temperature ionic liquids, T. Hirade, *AIP Conf. Proc.* 2182, 030007 (2019).

9) Detector identification by waveform shape analysis for effective data acquisition: Improvements in time resolution and count rate for positron annihilation age–momentum correlation measurement, T. Hirade, H. Ando, K. Manabe & D. Ueda, *Nucl. Inst. & Methods in Phys. Res., A* 931, 100 (2019).

10) TEM analysis of ion tracks and hillocks produced by swift heavy ions of different velocities in $Y_3Fe_5O_{12}$, N. Ishikawa, T. Taguchi, A. Kitamura, G. Szenes, M.E. Toimil-Molares & C. Trautmann, *J. Applied Phys.* 127, 055902 (2020).

11) Degradation prediction of a γ-ray radiation dosimeter using InGaP solar cells in a primary containment vessel of the Fukushima Daiichi Nuclear Power Station, Y. Okuno, M. Yamaguchi, N. Okubo & M. Imaizumi, *J. Nucl. Sci. Tech.* 57(4), 457 (2020).

12) Irradiation influence on swelling and corrosion behavior of ADS beam window materials, T91 Steels, in Lead Bismuth, N. Okubo & Y. Fujimura, *JPS Conf. Proc.* 28 (Proc. 14th Int. WS on Spallation Mater. Tech.), 071001 (2020).

13) Temperature dependence of ortho-Positronium Annihilation in Room Temperature Ionic Liquids, T. Hirade, K. Michishio, Y. Kobayashi & N. Oshima, *Acta Phys. Polonica A* 137(2), 109 (2020).

14) Study on loss-of-cooling and loss-of-coolant accidents in spent fuel pool, (1) Overview, Y. Kaji, Y. Nemoto, T. Nagatake, H. Yoshida, M. Tojo, D. Goto, S. Nishimura, H. Suzuki, M. Yamato & S. Watanabe, *Proc. ICONE27*, 1343 (2019).

15) Study on loss-of-cooling and loss-of-coolant accidents in spent fuel pool, (2) Fuel cladding oxidation, Y. Nemoto, Y. Kaji, T. Kanazawa, K. Nakashima & M. Tojo, *Proc. ICONE27*, 1345 (2019).

16) Study on loss-of-cooling and loss-of-coolant accidents in spent fuel pool, (3) Thermal-hydraulics experiment by using simulated 4×4 fuel bundle for constructing validation database, T. Nagatake, M. Shibata, H. Yoshida, Y. Nemoto & Y. Kaji, *Proc. ICONE27*, 1642 (2019).

17) Study on loss-of-cooling and loss-of-coolant accidents in spent fuel pool, (4) Investigation of fuel loading effects in BWR spent fuel rack, M.Tojo, T.Kanazawa, K.Nakashima, T.Iwamoto, K.Kobayashi, D.Goto, Y. Nemoto & Y.Kaji, *Proc. ICONE27*, 1477 (2019).

18) Study on loss-of-cooling and loss-of-coolant accidents in spent fuel pool, (5) Investigation of cooling effects of SFP spray and alternate water injection using MAAP code, S. Nishimura, M. Satake, Y. Nishi, Y. Nemoto & Y. Kaji, *Proc. ICONE27*, 1603 (2019).

19) Study on loss-of-cooling and loss-of-coolant accidents in spent fuel pool, (6) Analysis on oxidation behavior of fuel cladding tubes by the SAMPSON code, Y. Morita, H. Suzuki, M. Naitoh, Y. Nemoto & Y. Kaji, *Proc. ICONE27*, 1469 (2019).

20) Study on loss-of-cooling and loss-of-coolant accidents in spent fuel pool, (7) Analysis on effectiveness of spray cooling by the SAMPSON Code, H. Suzuki, Y. Morita, M. Naitoh, Y. Nemoto, T. Nagatake & Y. Kaji, *Proc. ICONE27*, 1475 (2019).

21) Study on loss-of-cooling and loss-of-coolant accidents in spent fuel pool, (8) Safety Margin of Spent Fuel in Large LOCA event by the Simple Assessment Method, T. Someya, H. Chitose, S. Watanabe, Y. Nemoto & Y. Kaji, *Proc. ICONE27*, 1153 (2019).

22) Development of cation and anion exchange membranes for saline water concentration using high-energy heavy-ion beams, S. Sawada, M. Yasukawa, H. Koshikawa, A. Kitamura, M. Higa & T. Yamaki, *Bull. Soc. Sea Water Sci. Jpn* 73(4), 208 (2019) (*in Japanese*).

23) Hydrogen desorption spectra from excess vacancy-type defects enhanced by hydrogen in tempered martensitic steel showing quasi-cleavage Fracture, K. Saito, T. Hirade & K. Takai, *Metal. Mater. Trans. A* 50(11), 5091 (2019).

24) Mechanism of hardening and damage initiation in oxygen embrittlement of body-centred-cubic niobium, P.-J. Yang, Q.-J. Li, T. Tsuru, S. Ogata, J.-W. Zhang, H.-W. Sheng, Z.-W. Shan, G. Sha, W.-Z.

Han, J. Li & E. Ma, *Acta Mater.* 168, 331 (2019).

25) First-principles modeling for dislocation motion of HEA alloys, T. Tsuru, M. Itakura, K. Yuge, Y. Aoyagi, T. Shimokawa, M. Kubo & S. Ogata, *Proc.*

ISAM-4 (4th International Symposium on Atomistic and Multiscale Modeling of Mechanics and Multiphysics), 1 (2019).

Patents

1) Okuno Y. & Okamoto T., "Radiation detector", *Japanese Patent Application* 2020-0062731 (2020.03.31)

2) Ueda M., Hayashi Y., Kawamura K., Irisawa E.,

Komatsu A., Okubo N., *et al.*, "Metal oxide thin film reduction sensor", *Japanese Patent Application* 2020-0062404 (2020.03.31)

Research Group for High Temperature Science on Fuel Materials

Papers

1) Observation of simulated fuel debris using synchrotron radiation, Y. Yoneda, M. Harada & M. Takano, *Trans. the Mater. Res. Soc. Jpn* 44(2), 61 (2019).

2) Thermodynamic approach for determination of fuel relocation condition in severe accident progression, A. Itoh, Y. Kobayashi, A. Suzuki, T. Sato, N. Shirasu, Y. Nagae & M. Kurata, *J. Nucl. Mater.* 529, 151925 (2020).

3) High-temperature interaction between

zirconium and UO_2, N. Shirasu, A. Suzuki, Y. Nagae & M. Kurata, *Proc. FDR2019 (Int. Topical WS on Fukushima Decommissioning Res.),* 1067 (2019).

4) Modelling of uranium dioxide interaction with zirconia at high temperature, A. Itoh, Y. Kobayashi, T. Sato, N. Shirasu, Y. Nagae, M. Kurata & A. Suzuki, *Proc. FDR2019 (Int. Topical WS on Fukushima Decommissioning Res.),* 1072 (2019).

JAEA Report

1) Development of module for ADS nitride fuel performance analysis, H. Shibata, H. Saito, H.

Hayashi & M. Takano, *JAEA-Data/Code 2019-023* (2020).

Nuclear Chemistry Division

Research Group for Radiochemistry

Papers

1) Extractions and spectroscopic studies of various metals with diglycolamide-type tridentate ligands, Y. Sasaki, M. Saeki & K. Yoshizuka, *Solvent Extr. Res. Dev., Jpn* 26(1), 21 (2019).

2) Impact of stoichiometry on the mechanism and kinetics of oxidative dissolution of UO_2 induced by H_2O_2 and γ-Irradiation, Y. Kumagai, A.B. Fidalgo & M. Jonsson, *J. Phys. Chem. C* 123(15), 9919 (2019).

3) Density functional theory (DFT)-based bonding analysis correlates ligand field strength with Ru-99 Mössbauer parameters of Ruthenium–Nitrosyl complexes, M. Kaneko, A. Kato, S. Nakashima & Y. Kitatsuji, *Inorg. Chem.* 58(20), 14024 (2019).

4) γ-Radiation and H_2O_2 induced oxidative

dissolution of uranium(IV) oxide in aqueous solution containing phthalic acid, Y. Kumagai & M. Jonsson, *Dalton Trans.* 49(6), 1907 (2020).

5) Preliminary study on separation of Dy and Nd by multi-step extraction using TDdDGA, Y. Sasaki, Y. Ban, K. Morita, M. Matsumiya, R. Ono & H. Shiroishi, *Solvent Extr. Res. Dev., Jpn* 27(1), 63 (2020).

6) Separation of palladium by solvent extraction with methylamino-bis-*N,N*-dioctylacetamide and direct electrodeposition from loaded organic phase, M. Matsumiya, Y. Song, Y. Tsuchida & Y. Sasaki, *Separation Purification Tech.* 234, 115841 (2020).

7) Optimization of sulfuric acid leaching of a Vietnamese rare earth concentrate, N.T. Hung,

L.B. Thuan, T. C. Thanh, <u>M. Watanabe</u>, H. Nhuan, D.V. Khoai, N.T. Thuy, N.V. Tung, N. Aoyagi, D.T.T. Tra, N.T. Minh, M.K. Jha, J.-Y. Lee, & R.K. Jyothi, *Hydrometallurgy* 191, 105195 (2020).

8) Spectroscopic studies of Mössbauer, infrared, and laser-induced luminescence for classifying rare-earth minerals enriched in iron-rich deposits, N. Aoyagi, T.T. Nguyen, <u>Y. Kumagai</u>, T.V. Nguyen, M. Nakada, Y. Segawa, H.T. Nguyen & T. Ba Le, *ACS Omega* 5(13), 7096 (2020).

9) Effect of H_2O_2 concentration on oxidative dissolution of UO_2, <u>Y. Kumagai</u>, *Biannual J. Jpn Soc. Radiation Chem.* 107, 77 (2019) (*in Japanese*).

10) Development of lanthanide and actinide studies toward interface chemistry using vibrational sum frequency generation spectroscopy, <u>R. Kusaka</u>, 放射化学 *Hosha kagaku* 41, 31 (2020) (*in Japanese*).

Patent

1) Suzuki T., <u>Sasaki Y.</u>, Morita K., Matsumura T. & Shimogouchi T., "Method of collecting platinum Group Element", *Japanese Patent* 6558566 (2019.07.26)

Research Group for Analytical Chemistry

Papers

1) External exposure dose estimation by electron spin resonance technique for wild Japanese macaque captured in Fukushima Prefecture, <u>T. Oka</u>, A. Takahashi, K. Koarai, Y. Mitsuyasu, Y. Kino, T. Sekine, Y. Shimizu, M. Chiba, T. Suzuki, K. Osaka, K. Sasaki, Y. Urushihara, S. Endo, M. Suzuki, H. Shinoda & M. Fukumoto, *Rad. Meas.* 134, 106315 (2020).

2) Thermodynamic study of the complexation of humic acid by calorimetry, S. Kimuro, A. Kirishima, <u>Y. Kitatsuji</u>, K. Miyakawa, D. Akiyama & N. Sato, *J. Chem. Thermodyn.* 132, 352 (2019).

3) Density functional theory (DFT)-based bonding analysis correlates ligand field strength with Ru-99 Mössbauer parameters of Ruthenium–

Nitrosyl complexes, M. Kaneko, A. Kato, S. Nakashima & <u>Y. Kitatsuji</u>, *Inorg. Chem.* 58(20), 14024 (2019).

4) Inverse magnetic susceptibility fabrics in pelagic sediment: Implications for magnetofossil abundance and alignment, Y. Usui, T. Yamazaki, <u>T. Oka</u> & Y. Kumagai, *J. Geophys. Res.: Solid Earth* 124(11), 10672 (2019).

5) Direct quantitation of Cs-135 in spent Cs adsorbent used for the decontamination of radiocesium-containing water by laser ablation inductively coupled plasma mass spectrometry, S. Asai, M. Ohata, <u>Y. Hanzawa</u>, T. Horita, T. Yomogida & Y. Kitatsuji, *Anal. Chem.* 92(4), 3276 (2020).

Environment and Radiation Sciences Division

Research Group for Environmental Science

Papers

1) Large-eddy simulation studies for predicting plume concentrations around nuclear facilities using an overlapping technique, <u>H. Nakayama</u> & T. Takemi, *Int. J. Environ. Pollution* 64(1/2/3), 125 (2018).

2) A new perspective on the Cs-137 retention mechanism in surface soils during the early stage after the Fukushima nuclear accident, <u>J. Koarashi</u>, S. Nishimura, M. Atarashi-Andoh, K. Muto & T. Matsunaga, *Sci. Reports* 9, 7034 (2019).

3) Development of regional downscaling capability in STEAMER ocean prediction system based on multi-nested ROMS model, <u>Y. Kamidaira</u>, H. Kawamura, T. Kobayashi & Y. Uchiyama, *J. Nucl. Sci. Tech.* 56(8), 752 (2019).

4) Characterizing vertical migration of Cs-137 in organic layer and mineral soil in Japanese forests: Four-year observation and model analysis, <u>K. Muto</u>, M. Atarashi-Andoh, T. Matsunaga & J. Koarashi, *J. Environ. Radioactivity* 208-209, 106040 (2019).

5) Predictability of a short-term emergency assessment system of the marine environmental radioactivity, <u>H. Kawamura</u>, Y. Kamidaira & T.

Kobayashi, *J. Nucl. Sci. Tech.* 57(4), 472 (2020).

6) Effect of dry-wet cycles on carbon dioxide release from two different volcanic ash soils in a Japanese temperate forest, H. Nagano, M. Atarashi-Andoh & J. Koarashi, *Soil Sci. Plant Nutrition* 65(5), 525 (2019).

7) Refinement of source term and atmospheric dispersion simulations of radionuclides during the Fukushima Daiichi Nuclear Power Station accident, H. Terada, H. Nagai, K. Tsuduki, A. Furuno, M. Kadowaki & T. Kakefuda, *J. Environ. Radioactivity* 213, 106104 (2020).

8) Processes affecting land-surface dynamics of I-129 impacted by atmospheric I-129 releases from a spent nuclear fuel reprocessing plant, M. Ota, H. Terada, H. Hasegawa & H. Kakiuchi, *Sci. the Total Environ.* 704, 135319 (2020).

9) Atmospheric-dispersion database system that can immediately provide calculation results for various source term and meteorological conditions, H. Terada, H. Nagai, A. Tanaka, K. Tsuduki & M. Kadowaki, *J. Nucl. Sci. Tech.* 57(6), 745 (2020).

10) Marine radionuclide transport modelling: Recent developments, problems and challenges, R. Periáñez, R. Bezhenar, I. Brovchenko, C. Duffa, M. Iosjpe, K.T. Jung, K.O. Kim, T. Kobayashi, L. Liptak, A.Little, V. Maderich, P. McGinnitym B.I. Min, H. Nies, I. Osvath, K.S. Suh & G. de With, *Environ. Modelling & Software* 122, 104523 (2019).

11) Repeatability and reproducibility of measurements of low dissolved radiocesium concentrations in freshwater using different pre-concentration methods, M. Kurihara, T. Yasutaka, T. Aono, N. Ashikawa, H. Ebina, T. Iijima, K. Ishimaru, R. Kanai, Z. Karube, Y. Konnai, T. Kubota, Y. Maehara, T. Maeyama, Y. Okizawa, H. Ota, S. Otosaka, A. Sakaguchi, H. Tagomori, K. Taniguchi, M. Tomita, H. Tsukada, S. Hayashi, S.y. Lee, S. Miyazu, M. Shin, T. Nakanishi, T. Nishikiori, Y. Onda, T. Shinano & H. Tsuji, *J. Radioanal. Nucl. Chem.* 322(2), 477 (2019).

12) Carbon dioxide balance in early-successional forests after forest fires in interior Alaska, M. Ueyama, H. Iwata, H. Nagano, N. Tahara, C. Iwama & Y. Harazono, *Agri. Forest Meteor.* 275, 196 (2019).

13) Development of field estimation technique and improvement of environmental tritium behavior Model, S. Yokoyama, T. Takahashi, M. Ota, H. Kakiuchi, S. Sugihara, S. Hirao, N. Momoshima, T. Tamari, N. Shima, M. Atarashi-Andoh, S. Fukutani, S. Nakasoe, M. Furukawa, M. Tanaka & N. Akata, *Plasma Fusion Res.* 14, 3405099 (2019).

14) Vertical distributions of Iodine-129 and iodide in the Chukchi Sea and Bering Sea, K. Miwa, H. Obata & T. Suzuki, *J. Nucl. Sci. Tech.* 57(5), 537 (2020).

15) Seven-year temporal variation of Cesium-137 discharge inventory from the port of Fukushima Dai-ichi Nuclear Power Plant: Continuous monthly estimation of Cesium-137 discharge in the period from April 2011 to June 2018, M. Machida, S. Yamada, A. Iwata, S. Otosaka, T. Kobayashi, M. Watanabe, H. Funasaka & T. Morita, *Trans. the Atomic Energy Soc. Jpn* 18(4), 226 (2019) (*in Japanese*).

16) Intercomparison of numerical atmospheric dispersion prediction models for emergency response to emissions of radionuclides with limited source information in the Fukushima Dai-ichi nuclear power plant accident, T. Iwasaki, T.T. Sekiyama, T. Nakajima, A. Watanabe, Y. Suzuki, H. Kondo, Yu Morino, H. Terada, H. Nagai, M. Takigawa, H. Yamazawa, D. Quélo & A. Mathieu, *Atmospheric Environ.* 214, 116830 (2019).

17) Wintertime grassland dynamics may influence belowground biomass under climate change: a model analysis, G. Katata, R. Grote, M. Mauder, M.J. Zeeman & M. Ota, *Biogeosci.* 17(4), 1071 (2020).

18) Reconstruction of residents' thyroid equivalent doses from internal radionuclides after the Fukushima Daiichi nuclear power station accident, T. Ohba, T. Ishikawa, H. Nagai, S. Tokonami, A. Hasegawa & G. Suzuki, *Sci. Reports* 10, 3639 (2020).

Book

1) 2 - Estimation of environmental releases of radioactive materials, M. Chino & H. Nagai, *Environmental Contamination from the Fukushima Nuclear Disaster Dispersion, Monitoring, Mitigation and Lessons Learned* / Cambridge Univ. Press, 50 (2019).

2) 8 - Dispersion modelling of radioactive materials, H. Nagai & H. Yamazawa, *Environmental Contamination from the Fukushima Nuclear Disaster: Dispersion, Monitoring, Mitigation and Lessons Learned* / Cambridge Univ. Press, 230 (2019).

Research Group for Radiation Transport Analysis

Papers

1) Correction notice to: Nowcast and forecast of galactic cosmic ray (GCR) and solar energetic particle (SEP) fluxes in magnetosphere and ionosphere – Extension of WASAVIES to Earth orbit, T. Sato, R. Kataoka, D. Shiota, Y. Kubo, M. Ishii, H. Yasuda, S. Miyake, Y. Miyoshi, H. Ueno & A. Nagamatsu, *J. Space Weather Space Climate* 9, A10 (2019).

2) Thick target neutron yields from 100- and 230-MeV/nucleon helium ions bombarding water, PMMA, and iron, P.-E. Tsai, L.H. Heilbronn, B.-L. Lai, Y. Iwata, T. Murakami & R.-J. Sheu, *Nucl. Inst. & Methods in Phys. Res., B* 449, 62 (2019).

3) Development of a function calculating internal dose coefficients based on ICRP 2007 Recommendations, K. Manabe, K. Sato & F. Takahashi, *BIO Web of Conf.* 14, 03011 (2019).

4) Estimating internal dose coefficients of short-lived radionuclides in accordance with ICRP 2007 recommendations, K. Manabe, K. Sato & F. Takahashi, *J. Nucl. Sci. Tech.* 56(5), 385 (2019).

5) Intensity modulated radiation fields induce protective effects and reduce importance of dose-rate effects, Y. Matsuya, S.J. McMahon, M. Ghita, Y. Yoshii, T. Sato, H. Date & K.M. Prise, *Sci. Reports* 9, 9483 (2019).

6) DNA damage induction during localized chronic exposure to an insoluble radioactive microparticle, Y. Matsuya, Y. Satou, N. Hamada, H. Date, M. Ishikawa & T. Sato, *Sci. Reports* 9, 10365 (2019).

7) Dosimetric dependence of ocular structures on eye size and shape for external radiation fields of electrons, photons, and neutrons, T. Furuta, D. El Basha, S. S R Iyer, C. M Correa Alfonso & W. E Bolch, *J. Radiol. Prot.* 39(3), 825 (2019).

8) Modeling of yield estimation for DNA strand breaks based on Monte Carlo simulations of electron track structure in liquid water, Y. Matsuya, T. Kai, Y. Yoshii, Y. Yachi, S. Naijo, H. Date & T. Sato, *J. Applied Phys.* 126(12), 124701 (2019).

9) Depth profiles of energy deposition near incident surface irradiated with swift heavy ions, T. Ogawa, N. Ishikawa & T. Kai, *Nucl. Inst. & Methods in Phys. Res., B* 461, 272 (2019).

10) Prediction of scintillation light yield based on track-structure simulation, T. Ogawa, T. Sato & T. Yamaki, *Biannual J. Jpn Soc. Radiation Chem.* 108, 11 (2019) (*in Japanese*).

11) Measurement of defect-induced electrical resistivity change of tungsten wire at cryogenic temperature using high-energy proton irradiation, Y. Iwamoto, M. Yoshida, H. Matsuda, S. Meigo, D. Satoh, H. Yashima, A. Yabuuchi, A. Kinomura & T. Shima, *JPS Conf. Proc.* 28, 061003 (2020).

12) A simplified cluster analysis of electron track structure for estimating complex DNA damage Yields, Y. Matsuya, T. Nakano, T. Kai, N. Shikazono, K. Akamatsu, Y. Yoshii & T. Sato, *Int. J. Molecular Sci.* 21(5), 1701 (2020).

13) Analysis of the high-dose-range radioresistance of prostate cancer cells, including cancer stem cells, based on a stochastic model, R. Saga, Y. Matsuya, R. Takahashi, K. Hasegawa, H. Date & Y. Hosokawa, *J. Radiat. Res.* 60(3), 298 (2019).

14) Cathodoluminescence induced in oxides by high-energy electrons: Effects of beam flux, electron energy, and temperature, J.-M. Costantini, T. Ogawa, AKM Saiful I. Bhuian & K. Yasuda, *J. Lumin.* 208, 108 (2019).

15) Computation speeds and memory requirements of mesh-type ICRP Reference computational phantoms in Geant4, MCNP6, and PHITS, Y.S. Yeom, M.C. Han, C.s. Choi, H.g. Han, B.h. Shin, T. Furuta & C.H. Kim, *Health Phys.* 116(5), 664 (2019).

16) PARaDIM: A PHITS-based Monte Carlo tool for internal dosimetry with tetrahedral mesh computational phantoms, L.M. Carter, T.M. Crawford, T. Sato, T. Furuta, C.s. Choi, C.H. Kim, J.L. Brown, W.E. Bolch, P.B. Zanzonico & J.S. Lewis, *J. Nucl. Med.* 60(12), 1802 (2019).

17) Measurement of thermal neutron capture cross section of Ga-71 with dual monitor foils and covariance analysis, P. Panikkath, N. Otuka, Y. Iwamoto & P. Mohanakrishnan, *Eur. Phys. J. A* 55(6), 91 (2020).

18) Neutron-induced damage simulations: Beyond defect production cross-section, displacement per atom and iron-based metrics, J.-Ch. Sublet, I.P. Bondarenko, G. Bonny, J.L. Conlin, M.R. Gilbert, L.R. Greenwood, P.J. Griffin, P. Helgesson, Y. Iwamoto, V.A. Khryachkov, T.A. Khromyleva, A.Yu. Konobeyev, N. Lazarev, L. Luneville, F. Mota, C.J. Ortiz, D. Rochman, S.P. Simakov, D. Simeone, H. Sjostrand, D. Terentyev & R. Vila, *Eur. Phys. J. Plus* 134(7), 350 (2019).

19) Impact of stellar superflares on planetary habitability, Y.A. Yamashiki, H. Maehara, V. Airapetian, Y. Notsu, T. Sato, S. Notsu, R. Kuroki,

34

K. Murashima, H. Sato, K. Namekata, T. Sasaki, T.B. Scott, H. Bando, S. Nashimoto, F. Takagi, C. Ling, D. Nogami & K. Shibata, *Astrophys. J.* 881(2), 114 (2019).

20) A biologically based mathematical model for spontaneous and ionizing radiation cataractogenesis, T. Sakashita, T. Sato & N. Hamada, *PLOS ONE* 14(8), e0221579 (2019).

21) Dosimetric impact of a new computational voxel phantom series for the Japanese atomic bomb survivors: Pregnant Females, C. Paulbeck, K. Griffin, C.s. Lee, H. Cullings, S.D. Egbert, S. Funamoto, T. Sato, A. Endo, N. Hertel & W.E. Bolch, *Rad. Res.* 191(5), 538 (2019).

22) Organ and detriment-weighted dose rate coefficients for exposure to radionuclide-contaminated soil considering body morphometries that differ from reference conditions: adults and children, C. Kofler, S. Domal, D. Satoh, S. Dewji, K. Eckerman & W.E. Bolch, *Rad. Environ. Biophys.* 58(4), 477 (2019).

23) Comparison of heavy-ion transport simulations: Collision integral with pions and Δ resonances in a box, A. Ono, J. Xu, M. Colonna, P. Danielewicz, C.M. Ko, M.B. Tsang, Y.-J. Wang, H. Wolter, Y.-X. Zhang, L.-W. Chen, D. Cozma, H. Elfner, Z.-Q. Feng, N. Ikeno, B.-A. Li, S. Mallik, Y. Nara, T. Ogawa, A. Ohnishi, D. Oliinychenko, J. Su, T.s. Song, F.-S. Zhang & Z. Zhang, *Phys. Rev. C* 100(4), 044617 (2019).

24) Track structure study for energy dependency of electrons and X-rays on DNA double-strand break induction, Y. Yachi, Y. Yoshii, Y. Matsuya, R. Mori, J. Oikawa & H. Date, *Sci. Reports* 9, 17649 (2019).

25) Measurement of displacement cross section of structural materials utilized in the proton accelerator facilities with the kinematic energy above 400MeV, S. Meigo, H. Matsuda, Y. Iwamoto, M. Yoshida, S. Hasegawa, F. Maekawa, H. Iwamoto, T. Nakamoto, T. Ishida & S. Makimura, *JPS Conf. Proc.* 28, 061004 (2020).

26) Anomalous radioisotope production for ^{68}ZnO using polyethylene by accelerator neutrons, K. Tsukada, Y. Nagai, S. Hashimoto, F. Minato, M. Kawabata, Y. Hatsukawa, K. Hashimoto, S. Watanabe, H. Saeki & S. Motoishi, *J. the Phys. Soc. Jpn* 89(3), 034201 (2020).

Books

1) 5.1.2 Properties and characteristics of radiations, F. Takahashi, 原子力のいまと明日 *Nuclear Energy's now and future (ed. by the Atomic Energy Soc. Jpn,)* / Maruzen, 106 (2019) (*in Japanese*).

2) 5.1.3 Units of radiation (radioactivity), F. Takahashi, 原子力のいまと明日 *Nuclear Energy's now and future (ed. by the Atomic Energy Soc. Jpn,)* / Maruzen, 109 (2019) (*in Japanese*).

3) Estimation of observables, T. Ogawa & Y. Iwamoto, 放射線遮蔽ハンドブック-応用編- *The handbook of radiation shielding -Advanced Edition-* / the Atomic Energy Soc. Jpn, 68 (2020) (*in Japanese*).

LWR Key Technology Development Division

Development Group for Thermal-Hydraulics Technology

Papers

1) Development of evaluation method for aerosol particle deposition in a reactor building based on CFD, N. Horiguchi, N. Miyahara, S. Uesawa, H. Yoshida & M. Osaka, *Proc. ICONE27*, 2158 (2019).

2) Observation of aerosol particle behavior near gas-liquid interface, S. Uesawa, N. Miyahara, N. Horiguchi, H. Yoshida & M. Osaka, *Proc. ICONE27*, 1972 (2019).

3) Development of numerical simulation method to evaluate detailed thermal hydraulics around beam window in ADS, S. Yamashita, T. Sugawara & H. Yoshida, *Proc. ICONE27*, 2019 (2019).

4) Study on loss-of-cooling and loss-of-coolant accidents in spent fuel pool, (3) Thermal-hydraulics experiment by using simulated 4×4 fuel bundle for constructing validation database, T. Nagatake, M. Shibata, H. Yoshida, Y. Nemoto & Y. Kaji, *Proc. ICONE27*, 1642 (2019).

5) Numerical simulation study of two-phase flow in 4x4 simulated fuel bundle, A. Ono, S. Yamashita, T. Suzuki & H. Yoshida, *Mechanical Eng. J.* 7(3), 19-00583 (2020).

6) Preliminary analysis of sodium experimental apparatus PLANDTL-2 to develop evaluation method for thermal hydraulics in reactor vessel of sodium-cooled fast reactor under decay heat removal system operation conditions, A. Ono, M. Tanaka, Y. Miyake, E. Hamase & T. Ezure, *Proc. ICONE27*, 2318 (2019).

7) Study on the two-phase flow in simulated LWR fuel bundle by CFD code, A. Ono, S. Yamashita, T. Suzuki & H. Yoshida, *Proc. NURETH-18 (18th International Topical Meeting on Nuclear Reactor Thermal Hydraulics)*, 666 (2019).

8) Development of fission product chemistry database ECUME for the LWR severe accident, S. Miwa, N. Miyahara, K. Nakajima, S. Nishioka, E. Suzuki, N. Horiguchi, J.-z. Liu, F. Miradji, J. Imoto, A. Mohamad, G. Takase, H. Karasawa & M. Osaka, *Proc. ICONE27*, 1993 (2019).

9) Development of fission product chemistry database ECUME for the LWR severe accident, S. Miwa, K. Nakajima, N. Miyahara, S. Nishioka, E. Suzuki, N. Horiguchi, J.z. Liu, F. Miradaiji, J. Imoto, A. Mohamad, G. Takase, H. Karasawa & M. Osaka, *Mechanical Eng. J.* 7(3), 19-00537 (2020).

10) Fuel debris' air cooling analysis using a lattice Boltzmann method, N. Onodera, Y. Idomura, T. Kawamura, S. Uesawa, S. Yamashita & H. Yoshida, *Proc. ICONE27*, 2306 (2019).

11) Study on loss-of-cooling and loss-of-coolant accidents in spent fuel pool, (1) Overview, Y. Kaji, Y. Nemoto, T. Nagatake, H. Yoshida, M. Tojo, D. Goto, S. Nishimura, H. Suzuki, M. Yamato & S. Watanabe, *Proc. ICONE27*, 1343 (2019).

12) Study on boiling behavior on vertical heating surface in pool boiling under higher pressure condition, A. Ono, S. Uesawa, M. Shibata, H. Yoshida & Y. Koizumi, *Proc. 56th National Heat Transfer Symposium*, B215 (2019) (*in Japanese*).

13) Effect of flow condition on sea salts deposition on boiling heat transfer surface, S. Uesawa, A. Ono, Y. Koizumi, M. Shibata & H. Yoshida, *Proc. 56th National Heat Transfer Symposium*, B135 (2019) (*in Japanese*).

14) Sea water flow boiling heat transfer involving sea salt deposition; Role of deposited sea salt, Y. Koizumi, S. Uesawa, A. Ono, M. Shibata & H. Yoshida, *Proc. JSME Thermal Eng. Conf. 2019*, G122 (2019) (*in Japanese*).

Patent

1) S. Uesawa, "Scrubbing method and system for polluted gas", *Japanese Patent Application* 2019- 162820 (2019.09.06)

Development Group for LWR Advanced Technology

Papers

1) Evaporation of ruthenium from simulated fission-produced alloy precipitates in a nuclear fuel, J.Z. Liu, N. Miyahara, S. Miwa, M. Takano, A. Hidaka & M. Osaka, *J. Nucl. Mater. 527*, 151819 (2019).

2) Boron chemistry during transportation in the high temperature region of a boiling water reactor under severe accident conditions, S. Miwa, G. Takase, J. Imoto, S. Nishioka, N. Miyahara & M. Osaka, *J. Nucl. Sci. Tech.* 57(3), 291 (2020).

3) An experimental investigation of influencing chemical factors on Cs-chemisorption behavior onto stainless steel, S. Nishioka, K. Nakajima, E. Suzuki & M. Osaka, *J. Nucl. Sci. Tech.* 56(11), 988 (2019).

4) Cesium chemisorbed species onto stainless steel surfaces: An atomistic scale study, F. Miradji, C. Suzuki, K. Nakajima & M. Osaka, *J. Phys. Chem. Solids* 136, 109168 (2020).

5) Development of fission product chemistry database ECUME for the LWR severe accident, S. Miwa, N. Miyahara, K. Nakajima, S. Nishioka, E. Suzuki, N. Horiguchi, J.-z. Liu, F. Miradji, J. Imoto, A. Mohamad, G. Takase, H. Karasawa & M. Osaka, *Proc. ICONE27*, 1993 (2019).

6) Development of fission product chemistry database ECUME for the LWR severe accident, S. Miwa, K. Nakajima, N. Miyahara, S. Nishioka, E. Suzuki, N. Horiguchi, J.z. Liu, F. Miradaiji, J. Imoto, A. Mohamad, G. Takase, H. Karasawa & M. Osaka, *Mechanical Eng. J.* 7(3), 19-00537 (2020).

7) Development of container using plasma sprayed and laser treated material for sulfuric acid decomposition of Ttermochemical water-splitting Iodine-sulfur Process, I. Ioka, Y. Kuriki, J. Iwatsuki, S. Kubo, Y. Inagaki & N. Sakaba, *Proc. ICONE27*, 2045 (2019).

8) Study of container using hybrid technique for sulfuric acid decomposition of thermochemical water-splitting iodine-sulfur process, I. Ioka, J. Iwatsuki, Y. Kuriki, D. Kawai, H. Yokota, S. Kubo, Y. Inagaki & N. Sakaba, *Mechanical Eng. J.* 7(3), 19-00377 (2020).

9) Study on chemisorption model of cesium hydroxide onto stainless steel type 304, <u>K. Nakajima</u>, S. Nishioka, E. Suzuki & M. Osaka, *Proc. ICONE27*, 2117 (2019).

10) Overview of accident-tolerant fuel R&D program in Japan, <u>S. Yamashita</u>, I. Ioka, Y. Nemoto, T. Kawanishi, M. Kurata, Y. Kaji, T. Fukahori, T. Nozawa, D. Sato, N. Murakami, H. Sato, T. Kondo, K. Sakamoto, K. Kusagaya, S. Ukai, A. Kimura & A. Yamaji. *Proc. GLOBAL/Top Fuel 2019* (2019).

11) Low temperature heat capacity of $Cs_2Si_4O_9$, <u>E. Suzuki</u>, K. Nakajima, M. Osaka, Y. Ohishi, H. Muta & K. Kurosaki, *J. Nucl. Sci. Tech.* 57(7), 852 (2020).

12) Expansion of high temperature creep test data for failure evaluation of BWR lower head in severe accident, Y. Yamaguchi, J. Katsuyama, <u>Y. Kaji</u>, M. Osaka & Y.sh. Li, *Proc. ICONE27*, 1915 (2019).

13) Development of evaluation method for aerosol particle deposition in a reactor building based on CFD, N. Horiguchi, <u>N. Miyahara</u>, S. Uesawa, H. Yoshida & M. Osaka, *Proc. ICONE27*, 2158 (2019).

14) Experimental investigation on boron oxidative vaporization processes from zirconium-boron and iron-boron alloys in a high temperature steam atmosphere, <u>J. Imoto</u>, S. Miwa & M. Osaka, *Extended abst. FDR2019 (Int. Topical WS on Fukushima Decommissioning Res.)*, 1062 (2019).

15) Experimental study on Cs chemisorption behaviour onto stainless steel at around 873 K, <u>E. Suzuki</u>, G. Takase, K. Nakajima, S. Nishioka, N. Hashimoto, S. Isobe & M. Osaka, *Extended abst. FDR2019 (Int. Topical WS on Fukushima Decommissioning Res.)*, 1068 (2019).

16) Chemical trapping of Sr vapor species by Zircaloy cladding under a specific chemical condition, <u>A. Mohamad</u>, K. Nakajima, S. Miwa, M. Osaka, Y. Ohishi, H. Muta & K. Kurosaki, *Extended abst. FDR2019 (Int. Topical WS on Fukushima Decommissioning Res.)*, 1065 (2019).

17) Development of Out of Pile Test for SiC Cladding to Simulate DBA Conditions in PWRs, K. Furumoto, D. Sato, S. Watanabe, T. Yumura, M. Okamoto, <u>S. Yamashita</u> & T. Fukahori. *Proc. GLOBAL/Top Fuel 2019* (2019).

JAEA Report

1) Fission product chemistry database ECUME version 1.1, <u>Develop. G. for LWR Advanced Technology</u>, *JAEA-Data/Code 2019-017* (2020).

Book

1) Sub-sections 14.3.1 and 14.3.2 of "14 - Advances in fuel chemistry during a severe accident: Update after Fukushima Daiichi Nuclear Power Station (FDNPS) accident", <u>M. Osaka</u>, *Advances in Nuclear Fuel Chemistry* / Elsevier (2020).

Partitioning and Transmutation Technology Division

Research Group for Partitioning

Papers

1) Extraction of trivalent rare earths and minor actinides from nitric acid with *N,N,N',N'*-tetradodecyldiglycolamide (TDdDGA) by using mixer-settler extractors in a hot cell, <u>Y. Ban</u>, H. Suzuki, S. Hotoku, T. Kawasaki, H. Sagawa, N. Tsutsui & T. Matsumura, *Solvent Extr. Ion Exch.* 37(1), 27 (2019).

2) Effects of diluents on the separation of minor actinides from lanthanides with tetradodecyl-1,10-phenanthroline-2,9-diamide from Nitric Acid Medium, <u>N. Tsutsui</u>, Y. Ban, H. Suzuki, M. Nakase, S. Ito, Y. Inaba, T. Mmatsumura & K. Takeshita, *Analytical Sci.* 36(2), 241 (2020).

3) Minor actinides separation by *N,N,N',N',N'',N''*-hexaoctyl nitrilotriacetamide (HONTA) using mixer-settler extractors in a hot cell, <u>Y. Ban</u>, H. Suzuki, S. Hotoku, N. Tsutsui, Y. Tsubata & T. Matsumura, *Solvent Extr. Ion Exch.* 37(7), 489 (2019).

4) Sorption properties of aluminum hexacyanoferrate for platinum group elements, <u>R. Mishima</u>, Y. Inaba, S. Tachioka, M. Harigai, S.

Watanabe, J. Onoe, M. Nakase, T. Matsumura & K. Takeshita, *Chem. Lett.* 49(1), 83 (2020).

5) Direct temperature-swing extraction of rare-earth elements from acidic solution using the hydrophobic interactions of poly (N-isopropylacrylamide) with diglycolamide-typed ligands, K. Saga, H. Suzuki, T. Mastumura & T. Tsukahara, *Analytical Sci.* 35(4), 461 (2020).

6) A review of separation processes proposed for advanced fuel cycles based on technology readiness level assessments, P. Baron, S.M. Cornet, E.D. Collins, G. DeAngelis, G. Del Cul, Yu. Fedorov, J.P. Glatz, V. Ignatiev, T. Inoue, A. Khaperskaya, I.T. Kim, M. Kormilitsyn, T. Koyama, J.D. Law, H.S. Lee, K. Minato, Y. Morita, J. Uhlíř, D. Warin & R.J. Taylor, *Prog. Nucl. Energy* 117, 103091 (2019).

7) Zr Separation from high level liquid waste with a novel hydroxyacetoamide type extractant, K. Morita, H. Suzuki, T. Matsumura, Y. Takahashi, T. Omori, M. Kaneko & K. Asano, *Proc. GLOBAL/Top Fuel 2019* (2019).

8) Extraction separation of minor actinides and lanthanides by 1,10-Phenanthroline-2,9-diamide with phenyl group in nitric acid systems, N. Tsutsui, M. Nakase, S. Ito, Y. Ban, T. Matsumura & K. Takeshita, *Proc. GLOBAL/Top Fuel 2019* (2019).

9) Development of SELECT process for minor actinides partitioning from high level waste, T.

Matsumura, 機能材料 *Function & materials* Jan. 2020 / 40(1), 60 (2020) (*in Japanese*).

10) Separation and recovery of raremetals using the hydrophiric extraction with phase transfer phenomena, T. Tsukahara, H. Suzuki, T. Matsumura & K. Saga, 分離技術 *Separation process eng.* 49(4), 29 (2019) (*in Japanese*).

11) Separation process of long-lived fission products from high-level radioactive wastes, Y. Takahashi, T. Omori, E. Murata, Y. Yamashita, M. Kaneko, K. Asano, K. Morita, H. Suzuki & T. Matsumura, *Proc. GLOBAL/Top Fuel 2019* (2019).

12) Characterization of HONTA/SiO$_2$-P adsorbent for MA(III)/Ln(III) separation flow-sheet, M. Takeuchi, S. Watanabe, Y. Sano, H. Kofuji, H. Suzuki & T. Matsumura, *Proc. GLOBAL/Top Fuel 2019* (2019).

13) Influence of filling fraction of simulated high-level waste on consistency in flexible waste management system, A. Suzuki, Y. Endo, T. Fukasawa, Y. Muroya & T. Matsumura, *Proc. GLOBAL/Top Fuel 2019* (2019).

14) No secondary waste recycle technology for raremetals using the hydrophiric extraction with phase transfer phenomena, T. Tsukahara, K. Saga, H. Suzuki & T. Matsumura, クリーンテクノロジー *Clean technology* Dec. 2019 / 29(12), 4 (2019) (*in Japanese*).

JAEA Report

1) Evaluation of decay heat value from high-level liquid waste; Data for safety assessment of

partitioning process, Y. Morita & Y. Tsubata, *JAEA-Data/Code 2019-015* (2020).

Patents

1) Matsumura T., Sano Y., Tsubata Y., Koyama S., Yamamura T., Suzuki T., Takao K., Kani Y., Takahashi Y., Oyama S., Komamine S., Fujita R. & Ozawa M., "Process for treating insoluble residue", *Japanese Patent* 6515369 (2019.04.26)

2) Suzuki H., Matsumura T., Urabe S., Kurosawa T., Kawasaki T., Kunii S., Yoshida T., Narita K. & Tanaka M., "Method of extracting Actinoids and/or Lanthanoids", *Japanese Patent* 6521286 (2019.05.10)

3) Suzuki H., Matsumura T., Kunii S. & Yoshida T., "Scandium and/or Lanthanoid extraction

method", *Japanese Patent* 6554745 (2019.07.19)

4) Suzuki T., Sasaki Y., Morita K., Matsumura T. & Shimogoucghi T., "Method of collecting platinum group element", *Japanese Patent* 6558566 (2019.07.26)

5) Suzuki H., Matsumura T., Kunii S. & Yoshida T., "Extraction method for actinoid and/or rare earth", *Japanese Patent* 6635259 (2019.12.27)

6) Matsumura T. & Suzuki H., "Extraction method for americium", *Japanese Patent Application* 2019-151070 (2019.08.21)

Research Group for Nuclear Transmutation System

Papers

1) Application of linear combination method to

pulsed neutron source measurement at Kyoto

University critical assembly, <u>R. Katano</u>, M. Yamanaka & C.H. Pyeon, *Nucl. Sci. Eng.* 193(12), 1394 (2019).

2) Systematic measurements and analyses for lead void reactivity worth in a plutonium core and two uranium cores with different enrichments, <u>M. Fukushima</u>, J. Goda, A. Oizumi, J. Bounds, T. Cutler, T. Grove, D. Hayes, J. Hutchinson, G. McKenzie, A. McSpaden, R. Sanchez, J. Walker & K. Tsujimoto, *Nucl. Sci. Eng.* 194(2), 138 (2020).

3) Area ratio method via linear combination of the neutron counts in pulsed neutron experiment., <u>R. Katano</u>, *Proc. ICONE27*, 1327 (2019).

4) Measurement of prompt neutron decay constant with spallation neutrons at Kyoto University Critical Assembly using linear combination method, <u>R. Katano</u>, M. Yamanaka & C.H. Pyeon, *J. Nucl. Sci. Tech.* 57(2), 169 (2020).

5) First nuclear transmutation of Np-237 and Am-241 by accelerator-driven system at Kyoto University Critical Assembly, C.H. Pyeon, M. Yamanaka, <u>A. Oizumi</u>, M. Fukushima, G. Chiba, K. Watanabe, T. Endo, W.G. Van Rooijen, K. Hashimoto, A. Sakon, N. Aizawa, Y. Kuriyama, T. Uesugi & Y. Ishi, *J. Nucl. Sci. Tech.* 56(8), 684 (2019).

6) Immortal experimental loop at JAEA - Post-

JAEA Report

1) Development of prototype for TEF-T integral control system of J-PARC, K. Sakai, H. Obayashi, S.

process and validation, <u>N. Watanabe</u>, H. Obayashi, T. Sugawara, T. Sasa, K. Nishihara & D. Castelliti, *Proc. NURETH-18 (18th International Topical Meeting on Nuclear Reactor Thermal Hydraulics)*, 248 (2019).

7) Design of accelerator-driven system consistent to partitioning technology, <u>T. Sugawara</u>, Y. Ban, R. Katano, H. Tateno & K. Nishihara, *Proc. Int. Conf. the Management of Spent Fuel from Nuclear Power Reactors* (2019).

8) PR4-3 measurement of MA reaction rates under sub-critical condition with spallation neutron source in A-core of KUCA for ADS, <u>A. Oizumi</u>, M. Fukushima, K. Tsujimoto, G. Chiba, M. Yamanaka, T. Sano & C.H. Pyeon, *KURNS PROGRESS REPORT 2018*, 38 (2019).

9) CO3-7 sample worth measurements with systematically changed mixing ratios of Lead and Bismuth in A-core of KUCA for ADS, <u>M. Fukushima</u>, A. Oizumi, M. Yamanaka & C.H. Pyeon, *KURNS PROGRESS REPORT 2018*, 143 (2019).

10) Current status of R&D and PIE program for ADS material development in JAEA, S. Saito, N. Okubo, H. Obayashi, T. Wan, <u>T. Sugawara</u>, T. Sasa & F. Maekawa, *JPS Conf. Proc.* 28 (Proc. 14th Int. WS on Spallation Mater. Tech.), 071003 (2020).

Saito, T. Sasa, <u>T. Sugawara</u> & A. Watanabe, *JAEA-Technology 2019-009* (2019) (*in Japanese*).

Research Group for MA Transmutation Fuel Cycle

Papers

1) Material balance evaluation of pyroprocessing for minor actinide transmutation nitride fuel, H. Tateno, <u>T. Sato</u>, Y. Tsubata & H. Hayashi, *J. Nucl. Sci. Tech.* 57(3), 224 (2020).

2) Recent progress on development of

pyroprocessing technology for minor actinide transmutation nitride fuels, <u>H. Hayashi</u>, T. Sato, H. Tateno, S. Akashi, H. Shibata & Y. Tsubata, *Proc. GLOBAL/Top Fuel 2019* (2019).

Nuclear Science and Engineering Center

Papers

1) Enhancing emergency response in the field based on analysis of workload distribution at Fukushima Daiichi Nuclear Power Station, A. Yoshizawa, <u>K. Oba</u> & M. Kitamura, *Trans. the Atomic Energy Soc. Jpn* 18(2), 55 (2019) (*in*

Japanese).

2) Let's aim at AESJ without Ethics Committee, <u>K. Oba</u>, *J. the Atomic Soc. Jpn* 61(4), 347 (2019) (*in Japanese*).